Clinical Science (2021) **135** 515–534
https://doi.org/10.1042/CS20201122

Research Article

Acid sphingomyelinase promotes SGK1-dependent vascular calcification

Trang Thi Doan Luong[1], Rashad Tuffaha[2], Mirjam Schuchardt[3], Barbara Moser[1], Nadeshda Schelski[4], Beate Boehme[4], Can Gollmann-Tepeköylü[5], Clara Schramm[6], Johannes Holfeld[5], Burkert Pieske[4,7,8,9], Erich Gulbins[10], Markus Tölle[3], Markus van der Giet[3], Florian Lang[2], Kai-Uwe Eckardt[3], Jakob Voelkl[1,3,9] and Ioana Alesutan[1]

[1]Institute for Physiology and Pathophysiology, Johannes Kepler University Linz, Linz, Austria; [2]Department of Physiology I, Eberhard-Karls University, Tübingen, Germany; [3]Department of Nephrology and Medical Intensive Care, Charité – Universitätsmedizin Berlin, corporate member of Freie Universität Berlin, Humboldt-Universität zu Berlin, and Berlin Institute of Health, Berlin, Germany; [4]Department of Internal Medicine and Cardiology, Campus Virchow-Klinikum, Charité – Universitätsmedizin Berlin, Berlin, Germany; [5]University Clinic of Cardiac Surgery, Medical University of Innsbruck, Innsbruck, Austria; [6]Division of Pathophysiology, Institute for Physiology and Pathophysiology, Johannes Kepler University Linz, Linz, Austria; [7]Berlin Institute of Health (BIH), Berlin, Germany; [8]Department of Internal Medicine and Cardiology, German Heart Center Berlin (DHZB), Berlin, Germany; [9]DZHK (German Centre for Cardiovascular Research), Partner Site Berlin, Berlin, Germany; [10]Institute of Molecular Biology, University Hospital Essen, University of Duisburg-Essen, Essen, Germany

Correspondence: Jakob Voelkl (jakob.voelkl@jku.at)

In chronic kidney disease (CKD), hyperphosphatemia is a key factor promoting medial vascular calcification, a common complication associated with cardiovascular events and high mortality. Vascular calcification involves osteo-/chondrogenic transdifferentiation of vascular smooth muscle cells (VSMCs), but the complex signaling events inducing pro-calcific pathways are incompletely understood. The present study investigated the role of acid sphingomyelinase (ASM)/ceramide as regulator of VSMC calcification. *In vitro*, both, bacterial sphingomyelinase and phosphate increased ceramide levels in VSMCs. Bacterial sphingomyelinase as well as ceramide supplementation stimulated osteo-/chondrogenic transdifferentiation during control and high phosphate conditions and augmented phosphate-induced calcification of VSMCs. Silencing of serum- and glucocorticoid-inducible kinase 1 (SGK1) blunted the pro-calcific effects of bacterial sphingomyelinase or ceramide. Asm deficiency blunted vascular calcification in a cholecalciferol-overload mouse model and *ex vivo* isolated-perfused arteries. In addition, Asm deficiency suppressed phosphate-induced osteo-/chondrogenic signaling and calcification of cultured VSMCs. Treatment with the functional ASM inhibitors amitriptyline or fendiline strongly blunted pro-calcific signaling pathways *in vitro* and *in vivo*. In conclusion, ASM/ceramide is a critical upstream regulator of vascular calcification, at least partly, through SGK1-dependent signaling. Thus, ASM inhibition by repurposing functional ASM inhibitors to reduce the progression of vascular calcification during CKD warrants further study.

Introduction

The excessive risk of cardiovascular events in chronic kidney disease (CKD) is associated with medial vascular calcification [1,2]. This calcification is considered an active process involving transdifferentiation of vascular smooth muscle cells (VSMCs) into cells with osteoblast- and chondroblast-like properties [3,4]. These cells display increased expression of osteogenic transcription factors such as msh homeobox 2 (MSX2) and core-binding factor α1 (CBFA1) and subsequent expression of osteogenic enzymes including tissue-nonspecific alkaline phosphatase (ALPL), with a key role in producing a local pro-calcifying environment to allow vascular calcification [2,3]. Transdifferentiated VSMCs are able to augment vascular tissue calcification through mechanisms with similarities to physiological bone formation [5]. In CKD,

Received: 07 September 2020
Revised: 07 January 2021
Accepted: 21 January 2021

Accepted Manuscript online: 21 January 2021
Version of Record published: 03 February 2021

Clinical Science (2021) **135** 515–534
https://doi.org/10.1042/CS20201122

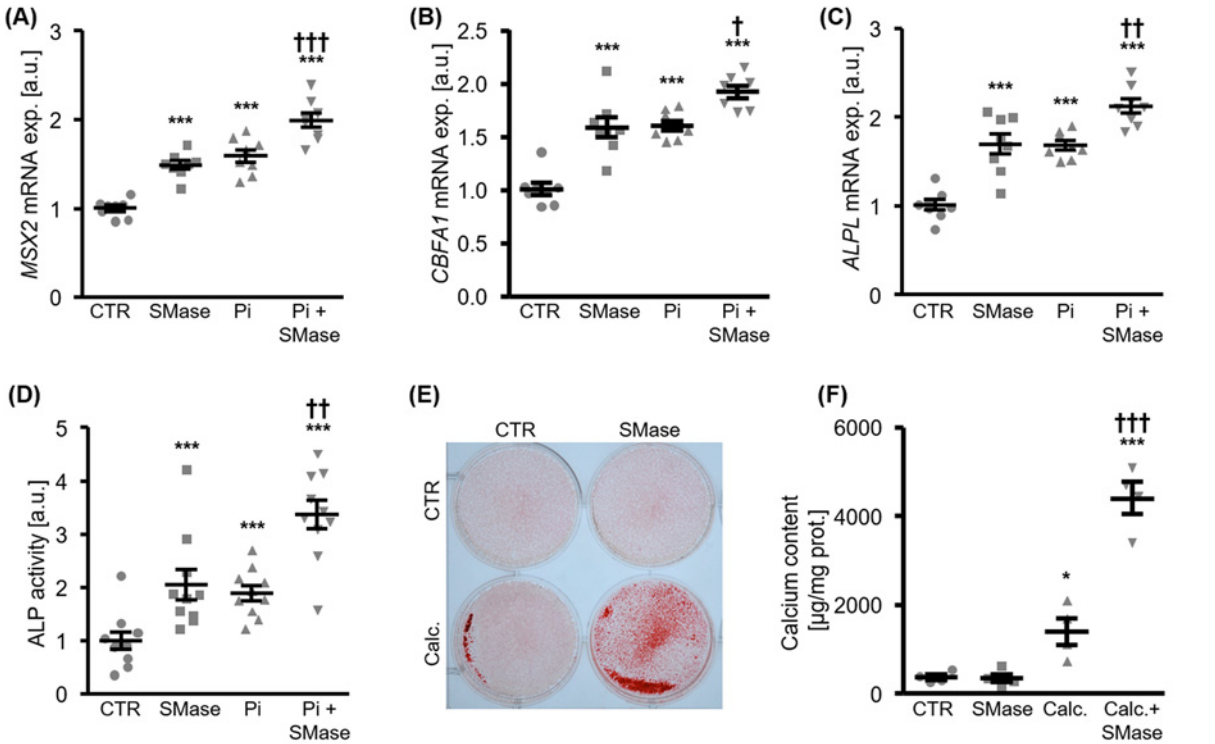

Figure 1. ASM promotes osteo-/chondrogenic transdifferentiation and aggravates phosphate-induced calcification of HAoSMCs

(**A–C**) Scatter dot plots and arithmetic means ± SEM (n=8; arbitrary units, a.u.) of *MSX2* (A), *CBFA1* (B) and *ALPL* (C) relative mRNA expression in HAoSMCs following treatment for 24 h with control (CTR), bacterial sphingomyelinase (SMase) or β-glycerophosphate (Pi) alone and together with bacterial sphingomyelinase (SMase). (**D**) Scatter dot plots and arithmetic means ± SEM (n=10, a.u.) of normalized ALP activity in HAoSMCs following treatment for 7 days with control (CTR), bacterial sphingomyelinase (SMase) or β-glycerophosphate (Pi) alone and together with bacterial sphingomyelinase (SMase). (**E**) Representative images showing Alizarin Red staining in HAoSMCs following treatment for 11 days with control (CTR), bacterial sphingomyelinase (SMase) or calcification medium (Calc.) alone and together with bacterial sphingomyelinase (SMase). The calcified areas are shown as red. (**F**) Scatter dot plots and arithmetic means ± SEM (n=4; µg/mg protein) of calcium content in HAoSMCs following treatment for 11 days with control (CTR), bacterial sphingomyelinase (SMase) or calcification medium (Calc.) alone and together with bacterial sphingomyelinase (SMase). *(P<0.05), ***(P<0.001) significant compared with control HAoSMCs; †(P<0.05), ††(P<0.01), †††(P<0.001) significant compared with Pi/Calc.-treated HAoSMCs.

phosphate is considered a key factor promoting VSMC osteo-/chondrogenic transdifferentiation and calcification via complex signaling pathways [3,6,7]. Activation of the transcription factor nuclear factor κ-light-chain-enhancer of activated B cells (NF-κB) by the serum- and glucocorticoid-inducible kinase 1 (SGK1) is described as critical signaling event promoting VSMC calcification [8], but the upstream regulators are still ill-defined [3]. VSMC calcification involves may involve processing of calcium-phosphate particles in lysosomes [9]. Lysosomal alkalinization is able to interfere with phosphate-induced VSMC osteo-/chondrogenic transdifferentiation [10].

Acid sphingomyelinase (ASM) is a ceramide-producing enzyme active at acidic pH [11], localized mainly in the lysosomes [12], but also secreted extracellularly [13], possibly involving lysosomal exocytosis [14]. Ceramides are sphingolipids, which can function as signaling molecules [15,16] with a critical role in vascular physiology and pathophysiology [13,17–19]. Ceramides are generated through hydrolysis of sphingomyelin by sphingomyelinases, and in addition through the salvage pathway or *de novo* synthesis [17,20]. Sphingomyelinases differ in their enzymatic properties and subcellular localization, which determine the signaling cascades and cellular processes regulated [13]. Moreover, various pathological stimuli may induce relocation of ASM to the plasma membrane producing ceramide-enriched cell membrane domains [16,21,22].

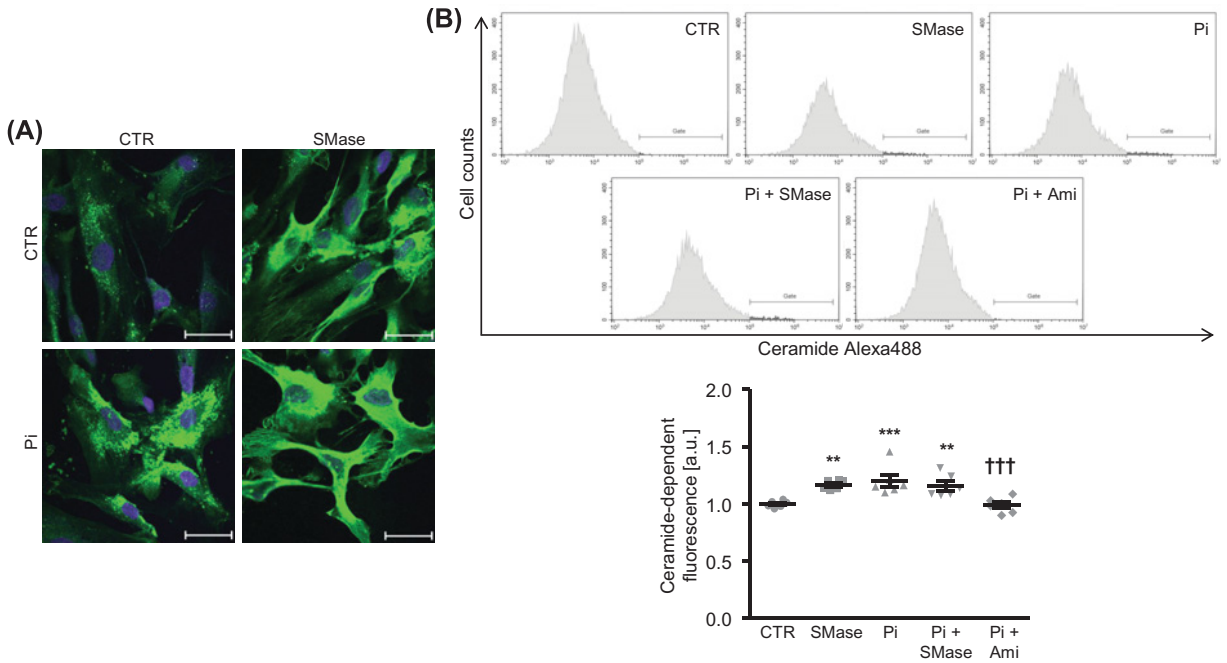

Figure 2. Phosphate increases ceramide levels in HAoSMCs

(**A**) Representative confocal microscopy images showing ceramide levels in HAoSMCs following treatment for 5 min with control (CTR), bacterial sphingomyelinase (SMase) or β-glycerophosphate (Pi) alone and together with bacterial sphingomyelinase (SMase). Ceramide: green labeling, nuclei: magenta labeling. Scale bar: 50 μm. (**B**) Representative histograms of flow cytometry analysis and scatter dot plots and arithmetic means ± SEM (n=6; arbitrary units, a.u.) of normalized ceramide-dependent fluorescence intensity in HAoSMCs following treatment for 5 min with control (CTR), bacterial sphingomyelinase (SMase) or β-glycerophosphate (Pi) alone and together with bacterial sphingomyelinase (SMase) or amitriptyline (Ami). **(P<0.01), ***(P<0.001) significant compared with control HAoSMCs; †††(P<0.001) significant compared with Pi-treated HAoSMCs.

Ceramides are also found in the circulation, and may be modified by diet [23]. Some plasma ceramides and especially ratios of ceramide species have been suggested as biomarkers for cardiovascular risk [24–26]. Increased plasma ceramide levels are observed in CKD patients [27]. ASM activation and ceramide accumulation have been suggested to contribute to endothelial dysfunction and atherosclerosis [28,29]. However, also atheroprotective effects of ASM were described [30,31]. Nonetheless, a possible involvement of ASM [32] and ceramide [33,34] in the signaling leading to vascular calcification is described.

We hypothesize that ASM activation and ceramide production may be induced by high phosphate conditions in VSMCs and ASM/ceramide may participate in the signaling promoting osteo-/chondrogenic transdifferentiation of VSMCs and, thus, contribute to the progression of vascular calcification. Therefore, the present study investigates the role and the underlying mechanisms of ASM in osteo-/chondrogenic transdifferentiation of VSMCs and vascular calcification during hyperphosphatemia.

Materials and methods

Cell culture of primary human aortic smooth muscle cells

Primary human aortic smooth muscle cells (HAoSMCs) (Thermo Fisher Scientific and Sigma–Aldrich) were routinely cultured (passages from 4 to 11) as described previously [35–37]. Where indicated, HAoSMCs were transfected with 10 nM SGK1 siRNA (ID no. s740) or 10 nM negative control siRNA (ID no. 4390843) using siPORT amine transfection agent (all from Thermo Fisher Scientific) [8]. HAoSMCs were transfected with 2 μg DNA encoding constitutively active $SGK1^{S422D}$ in pcDNA3.1 vector or empty vector as control [8,38] using X-tremeGENE HP DNA transfection reagent (Sigma–Aldrich). Cells were used 48 h after transfection and silencing or overexpression efficiency was verified by RT-PCR. HAoSMCs were treated with 0.01 U/ml sphingomyelinase (*Staphylococcus aureus*) (Enzo Life Sciences) [39], 10 μM C2-ceramide (stock in DMSO, Enzo Life Sciences) [33], 2 mM β-glycerophosphate (Sigma–Aldrich) [40–42], 5 μM amitriptyline (Sigma–Aldrich) [39], 5 μM fendiline (stock in DMSO, Santa Cruz

Clinical Science (2021) **135** 515–534
https://doi.org/10.1042/CS20201122

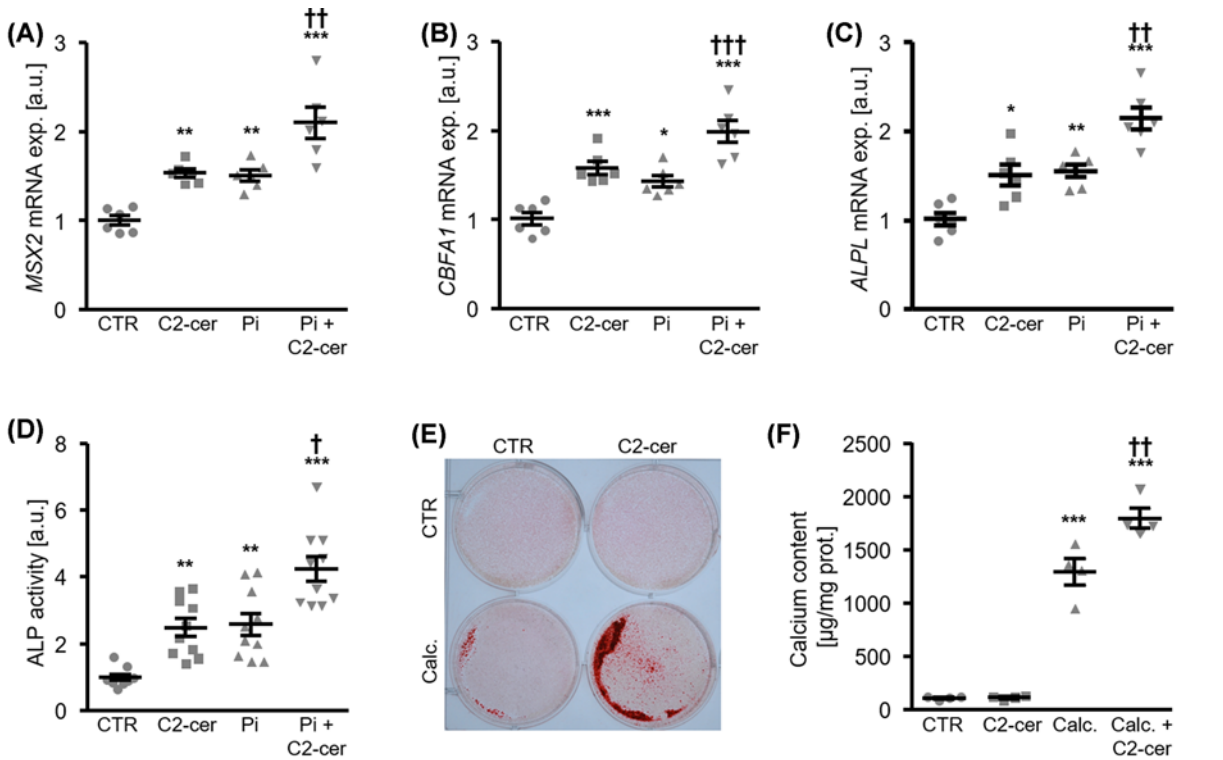

Figure 3. Ceramide stimulates osteo-/chondrogenic transdifferentiation and augments phosphate-induced calcification of HAoSMCs

(**A–C**) Scatter dot plots and arithmetic means ± SEM (n=6; arbitrary units, a.u.) of *MSX2* (A), *CBFA1* (B) and *ALPL* (C) relative mRNA expression in HAoSMCs following treatment for 24 h with control (CTR), C2-ceramide (C2-cer) or β-glycerophosphate (Pi) alone and together with C2-ceramide (C2-cer). (**D**) Scatter dot plots and arithmetic means ± SEM (n=10, a.u.) of normalized ALP activity in HAoSMCs following treatment for 7 days with control (CTR), C2-ceramide (C2-cer) or β-glycerophosphate (Pi) alone and together with C2-ceramide (C2-cer). (**E**) Representative images showing Alizarin Red staining in HAoSMCs following treatment for 11 days with control (CTR), C2-ceramide (C2-cer) or calcification medium (Calc.) alone and together with C2-ceramide (C2-cer). The calcified areas are shown as red. (**F**) Scatter dot plots and arithmetic means ± SEM (n=4; µg/mg protein) of calcium content in HAoSMCs following treatment for 11 days with control (CTR), C2-ceramide (C2-cer) or calcification medium (Calc.) alone and together with C2-ceramide (C2-cer). *(P<0.05), **(P<0.01), ***(P<0.001) significant compared with control HAoSMCs; †(P<0.05), ††(P<0.01), †††(P<0.001) significant compared with Pi/Calc.-treated HAoSMCs.

Biotechnology), 1 µM LY294002 (stock in DMSO, Enzo Life Sciences) and/or 100 nM wortmannin (stock in DMSO, Enzo Life Sciences) [43]. Equal amounts of vehicle were used as control. HAoSMCs were serum starved for 24 h prior to treatment with 15% uremic serum from hemodialysis patients (uremic serum, US) or control serum from matched healthy individuals (normal serum, NS) [8,41]. For analysis of mineralization, treatment with calcification medium containing 10 mM β-glycerophosphate and 1.5 mM $CaCl_2$ (Sigma–Aldrich) was used [37]. For long-term experiments, fresh medium with agents was added every 2–3 days.

Animal experiments

All animal experiments were approved by local authorities at University of Tuebingen, Charite Berlin and Medical University Vienna (Regierungspräsidium Tuebingen, LAGESO Berlin, BMBWF Vienna). Asm knockout mice ($Asm^{-/-}$) deficient in Asm activity and corresponding wild-type mice ($Asm^{+/+}$) were generated by gene targeting described previously [44,45]. Calcification was induced by high-dosed cholecalciferol treatment [46–48] in $Asm^{+/+}$ and $Asm^{-/-}$ mice and in C57BL/6 mice receiving water with control or supplemented with 100 mg/l amitriptyline (Sigma–Aldrich) or 67.5 mg/l fendiline (Santa Cruz Biotechnology) [49]. Mice were injected subcutaneously with 400000 IU/kg BW of cholecalciferol (Sigma–Aldrich) or vehicle for 3 days [8,37,47]. After 6 days, blood was obtained by retro-orbital puncture and animals were killed by cervical dislocation during inhalative isoflurane anesthesia and

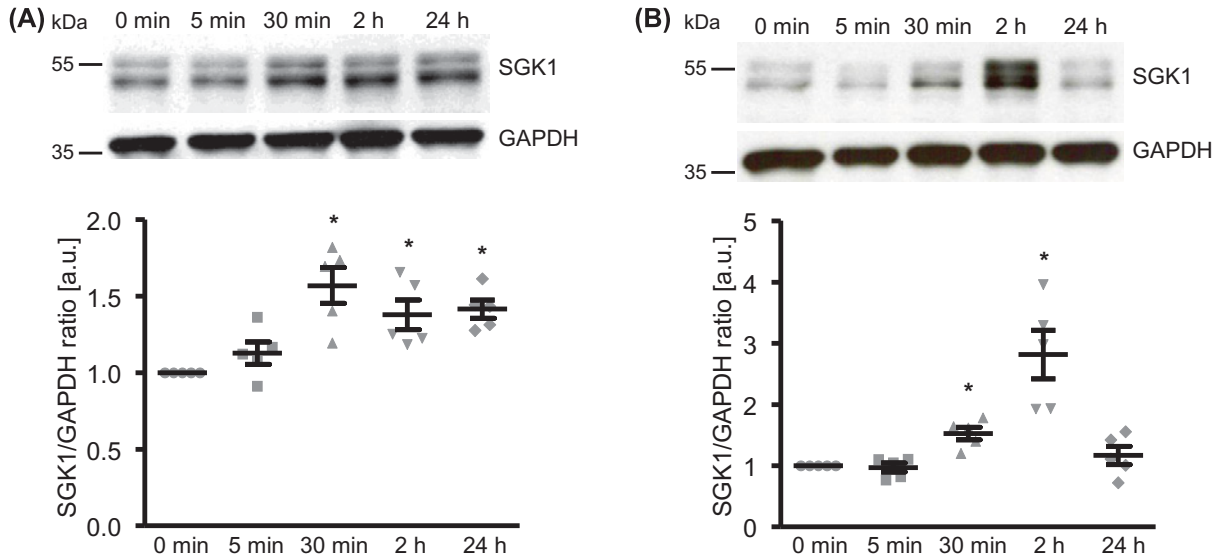

Figure 4. ASM and ceramide up-regulate SGK1 expression in HAoSMCs

(**A**) Representative Western blots and scatter dot plots and arithmetic means ± SEM (n=5; arbitrary units, a.u.) of normalized SGK1/GAPDH protein ratio in HAoSMCs following treatment for the indicated times with bacterial sphingomyelinase (SMase). (**B**) Representative Western blots and scatter dot plots and arithmetic means ± SEM (n=5; a.u.) of normalized SGK1/GAPDH protein ratio in HAoSMCs following treatment for the indicated times with C2-ceramide (C2-cer). *(P<0.05) significant compared with control HAoSMCs.

tissues snap-frozen in liquid nitrogen. A photometric method (FUJI FDC 3500i, Sysmex) was employed for determination of serum phosphate and calcium concentrations.

Cell culture of primary mouse aortic smooth muscle cells

Primary mouse aortic smooth muscle cells (MAoSMCs) were isolated from $Asm^{-/-}$ and $Asm^{+/+}$ mice and routinely cultured (passages from 3 to 7) as described previously [50]. MAoSMCs were treated with 2 mM β-glycerophosphate (Sigma–Aldrich) and/or 0.01 U/ml sphingomyelinase (*Staphylococcus aureus*) (Enzo Life Sciences). For analysis of mineralization, treatment with calcification medium containing 10 mM β-glycerophosphate and 1.5 mM $CaCl_2$ (Sigma–Aldrich) was used. For long-term experiments, fresh medium with agents was added every 2–3 days.

Isolated-perfused aortic tissue

For *ex vivo* perfusion, *Aorta thoracales* from $Asm^{-/-}$ and $Asm^{+/+}$ mice were used as described previously [51] with modifications for the mouse aorta instead of rat aorta. Briefly, a smaller perfusion chamber for a single mouse arterial perfusion was designed. In addition, the aortic preparation was refined for the smaller vessel type. For aorta clamping, blunted needles (26 gauge) were used. The aorta was perfused for 7 days under sterile conditions with calcification medium containing 5 mM sodium dihydrogen phosphate and 284 μM ascorbic acid. The medium was changed every 2 days. Afterwards, the aorta was collected for further analysis.

RNA isolation and RT-PCR

Total RNA was isolated from cells after 24 h of treatment and from aortic tissues by using TRIzol Reagent (Thermo Fisher Scientific). Reverse transcription of total RNA was performed by using oligo$(dT)_{12–18}$ primers and SuperScript III Reverse Transcriptase (Thermo Fisher Scientific). RT-PCR was performed in duplicate with iQ SYBR Green Supermix (Bio-Rad Laboratories) and CFX96 Real-Time PCR Detection System (Bio-Rad Laboratories). The specificity of the PCR products was confirmed by analysis of the melting curves. Relative mRNA fold changes were calculated by the $2^{-\Delta\Delta C_t}$ method using GAPDH as internal reference.

The following human primers were used (Thermo Fisher Scientific, 5′→3′) [8,40,52]:

ALPL fw: GGGACTGGTACTCAGACAACG;

Clinical Science (2021) **135** 515–534
https://doi.org/10.1042/CS20201122

ALPL rev: GTAGGCGATGTCCTTACAGCC;
BAX fw: CCCGAGAGGTCTTTTTCCGAG;
BAX rev: CCAGCCCATGATGGTTCTGAT;
BCL2 fw: GGTGGGGTCATGTGTGTGG;
BCL2 rev: CGGTTCAGGTACTCAGTCATCC;
CBFA1 fw: GCCTTCCACTCTCAGTAAGAAGA;
CBFA1 rev: GCCTGGGGTCTGAAAAAGGG;
GAPDH fw: GAGTCAACGGATTTGGTCGT;
GAPDH rev: GACAAGCTTCCCGTTCTCAG;
MSX2 fw: TGCAGAGCGTGCAGAGTTC;
MSX2 rev: GGCAGCATAGGTTTTGCAGC;
SGK1 fw: GCAGAAGAAGTGTTCTATGCAGT;
SGK1 rev: CCGCTCCGACATAATATGCTT.

The following mouse primers were used (Thermo Fisher Scientific, 5′→3′) [8,40,41,52]:

Alpl fw: TTGTGCCAGAGAAAGAGAGAGA;
Alpl rev: GTTTCAGGGCATTTTTCAAGGT;
Cbfa1 fw: AGAGTCAGATTACAGATCCCAGG;
Cbfa1 rev: AGGAGGGGTAAGACTGGTCATA;
Gapdh fw: AGGTCGGTGTGAACGGATTTG;
Gapdh rev: TGTAGACCATGTAGTTGAGGTCA;
Msx2 fw: TTCACCACATCCCAGCTTCTA;
Msx2 rev: TTGCAGTCTTTTCGCCTTAGC;
Sgk1 fw: CTGCTCGAAGCACCCTTACC;
Sgk1 rev: TCCTGAGGATGGGACATTTTCA.

Protein isolation and Western blotting

Following treatment for the indicated times, HAoSMCs were lysed with ice-cold IP lysis buffer supplemented with complete protease and phosphatase inhibitor cocktail (all from Thermo Fisher Scientific) [8,35,36]. Equal amounts of proteins were boiled in Roti-Load1 Buffer (Carl Roth) at 100°C for 10 min, separated on SDS/polyacrylamide gels and transferred to PVDF membranes. The membranes were incubated overnight at 4°C with primary antibodies: rabbit anti-SGK1 antibody (diluted 1:1000, #12103) or rabbit anti-GAPDH antibody (diluted 1:5000, #2118) and then with secondary anti-rabbit HRP-conjugated antibody (diluted 1:1000) (all from Cell Signaling) for 1 h at room temperature. For loading controls, the membranes were stripped in stripping buffer (Thermo Fisher Scientific) at room temperature for 10 min. Antibody binding was detected with ECL detection reagent (Thermo Fisher Scientific) and bands were quantified by using ImageJ software. Results are shown as the ratio of total protein to GAPDH, normalized to the control group.

Immunostaining and confocal microscopy

After 5 min of treatment, HAoSMCs were fixed with 4% paraformaldehyde/PBS for 20 min at room temperature. Slides were blocked with 5% normal goat serum in PBS for 1 h at room temperature and incubated with primary mouse anti-ceramide antibody (diluted 1:50 in PBS, Enzo Life Sciences) overnight at 4°C and then with anti-mouse Alexa 488-conjugated antibody (diluted 1:1000 in PBS, Thermo Fisher Scientific) for 1 h at room temperature [53]. Nuclei were stained using DRAQ5 dye (diluted 1:1000 in PBS, Biostatus) for 10 min at room temperature. The slides were mounted with Prolong Gold antifade reagent (Thermo Fisher Scientific). Negative controls were carried out simultaneously with all experiments by omitting incubation with primary antibody. Images were collected with a confocal imaging system (A1Rsi+, Nikon Instruments) using a 60× (Oil), 1.4 NA objective [37,41].

Flow cytometry analysis

HAoSMCs treated for 5 min or 24 h were harvested by trypsinization, blocked with 3% bovine serum albumin (BSA) in PBS for 15 min on ice and incubated with primary mouse anti-ceramide antibody (diluted 1:10 in 0.1% BSA/PBS, Enzo Life Sciences) for 45 min at 4°C and then with anti-mouse Alexa 488-conjugated antibody (diluted 1:50 in 0.1% BSA/PBS, Thermo Fisher Scientific) for 30 min at 4°C in the dark. Negative controls were carried out simultaneously

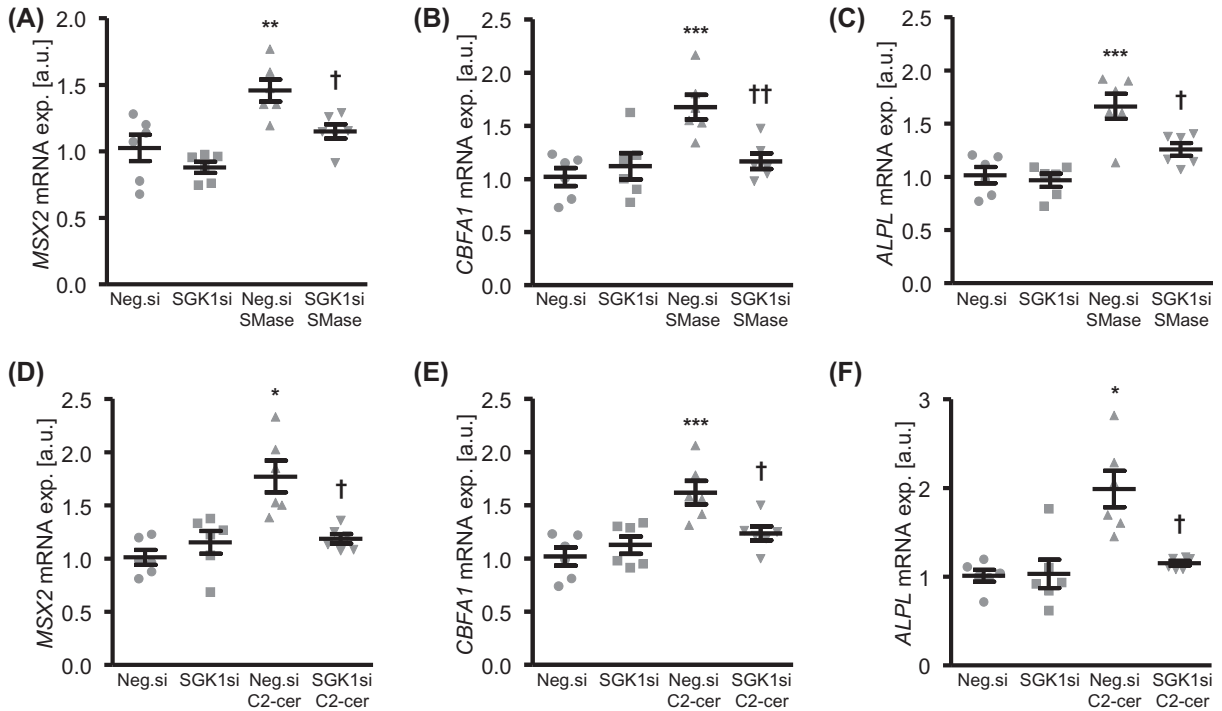

Figure 5. Silencing of SGK1 blunts ASM- and ceramide-induced osteo-/chondrogenic transdifferentiation of HAoSMCs

(**A–C**) Scatter dot plots and arithmetic means ± SEM (n=6; arbitrary units, a.u.) of *MSX2* (A), *CBFA1* (B) and *ALPL* (C) relative mRNA expression in HAoSMCs following transfection with negative control siRNA (Neg.si) or SGK1 siRNA (SGK1si) and treatment for 24 h with control or bacterial sphingomyelinase (SMase). (**D–F**) Scatter dot plots and arithmetic means ± SEM (n=6; a.u.) of *MSX2* (D), *CBFA1* (E) and *ALPL* (F) relative mRNA expression in HAoSMCs following transfection with negative control siRNA (Neg.si) or SGK1 siRNA (SGK1si) and treatment for 24 h with control or C2-ceramide (C2-cer). *(P<0.05), **(P<0.01), ***(P<0.001) significant compared with Neg.si-transfected HAoSMCs; †(P<0.05), ††(P<0.01) significant compared with Negsi-transfected and SMase/C2-cer-treated HAoSMCs.

with experiments by omitting incubation with primary antibody and with primary and secondary antibodies, respectively. Cells were measured by flow cytometry in FL-1 with an excitation wavelength of 488 nm and an emission wavelength of 530 nm using Cytoflex S flow cytometer (Beckman Coulter). Results are shown as median of relative fluorescence intensity of the gated ceramide-positive cell population, normalized to the control group.

ALP activity

ALP activity in HAoSMCs treated for 7 days was determined in cell lysates by using an ALP colorimetric assay kit (Abcam). Results are shown normalized to total protein concentration as measured by the Bradford assay (Bio-Rad Laboratories) [36,37,40] and to the control group.

Quantification of calcium content

Quantification of calcification in cells following treatment for 11 days was performed by incubation in 0.6 M HCl, overnight at 4°C. Aortic tissue was incubated in 0.6 M HCl, overnight at 37°C. Calcium levels in the supernatant was determined by using QuantiChrom Calcium assay kit (BioAssay Systems). Tissues or cells were lysed with 0.1 M NaOH/0.1% SDS and total protein concentration was measured by the Bradford assay (Bio-Rad Laboratories). Results are shown normalized to total protein concentration [8,37,54].

Staining procedures

After 11 days of treatment, cells were fixed with 4% paraformaldehyde/PBS and stained with 2% Alizarin Red (pH 4.5). Aortas were stained with 0.0016% Alizarin Red in 0.5% KOH. The calcified areas are shown as red [8,37,41]. Paraformaldehyde-fixed aortic tissue was cryoprotected in 30% sucrose, frozen in mounting medium (Tissue-Tek,

Clinical Science (2021) **135** 515–534
https://doi.org/10.1042/CS20201122

Sakura Finetek) and sectioned at 8-μm thickness on coated slides. Sections were stained for calcification by using the Von Kossa staining kit (Abcam). The calcified areas are shown as gray/black.

Statistics

Data are shown as scatter dot plots and arithmetic means ± SEM. *n* indicates the number of independent experiments performed at different cell passages or the number of mice examined. Normality was tested with Shapiro–Wilk test. Non-normal datasets were transformed (log, sqrt or reciprocal) prior to statistical testing to provide normality. Statistical testing was performed by one-way ANOVA followed by Tukey's HSD test for homoscedastic data or Games–Howell test for heteroscedastic data and by the Steel–Dwass method for non-normal data. Steel with control test was used for the time course experiments in cells. Two groups were compared by unpaired two-tailed *t* test. $P<0.05$ was considered statistically significant.

Results

Effects of ASM on osteo-/chondrogenic transdifferentiation and calcification of HAoSMCs

To investigate whether ASM impacts on osteo-/chondrogenic transdifferentiation and calcification of VSMCs, a first series of experiments was performed in HAoSMCs treated with sphingomyelinase isolated from *S. aureus* in the absence or presence of high phosphate levels. As a result, treatment with bacterial sphingomyelinase alone significantly up-regulated osteogenic markers *MSX2*, *CBFA1* and *ALPL* mRNA expression (Figure 1A–C) as well as ALP activity (Figure 1D) and, thus, induced osteo-/chondrogenic transdifferentiation of HAoSMCs. Moreover, bacterial sphingomyelinase significantly augmented phosphate-induced osteo-/chondrogenic transdifferentiation of HAoSMCs, as determined by the mRNA expression and activity of these markers (Figure 1A–D). In accordance, as shown by Alizarin Red staining (Figure 1E) and quantification of calcium content (Figure 1F), treatment with calcification medium triggered mineralization of HAoSMCs, effects significantly enhanced by addition of exogenous bacterial sphingomyelinase. Thus, bacterial sphingomyelinase promoted osteo-/chondrogenic transdifferentiation of VSMCs and aggravated phosphate-induced vascular calcification *in vitro*.

Regulation of ceramide levels in HAoSMCs

Next experiments explored the effects on ceramide levels in HAoSMCs. As indicated by confocal microscopy, bacterial sphingomyelinase increased ceramide abundance in HAoSMCs following 5 min of treatment (Figure 2A). In addition, ceramide levels were increased in HAoSMCs after 5 min of exposure to high phosphate concentrations (Figure 2A). These effects were confirmed by flow cytometry analysis. Treatment with bacterial sphingomyelinase or phosphate significantly up-regulated ceramide abundance in HAoSMCs after 5 min of treatment (Figure 2B), levels remaining significantly higher at 24 h following treatment (Supplementary Figure S1) as compared with control-treated HAoSMCs. Moreover, the functional ASM inhibitor amitriptyline significantly suppressed the increase in ceramide levels during high phosphate conditions, suggesting that ASM mediated, at least partly, phosphate-induced ceramide production (Figure 2B).

Effects of ceramide on osteo-/chondrogenic transdifferentiation and calcification of HAoSMCs

To determine whether ceramide regulates osteo-/chondrogenic transdifferentiation and calcification of VSMCs, HAoSMCs were treated with C2-ceramide alone or together with high phosphate concentrations. As illustrated in Figure 3A–D, exogenous C2-ceramide supplementation significantly up-regulated *MSX2*, *CBFA1* and *ALPL* mRNA expression and ALP activity in HAoSMCs. Moreover, the osteogenic markers mRNA expression and activity were all significantly higher in HAoSMCs treated with C2-ceramide together with phosphate than in HAoSMCs treated with phosphate alone (Figure 3A–D). Exogenous C2-ceramide augmented mineralization of HAoSMCs induced by calcification medium (Figure 3E,F). In addition, both, bacterial sphingomyelinase or C2-ceramide treatment significantly up-regulated *BAX*/*BCL2* relative mRNA expression ratio in HAoSMCs (Supplementary Figure S2), as indicator of increased apoptotic signaling, a process facilitating calcium-phosphate deposition.

Role of SGK1 in ASM/ceramide-induced osteo-/chondrogenic transdifferentiation of HAoSMCs

To elucidate the underlying mechanisms of ASM/ceramide-induced osteo-/chondrogenic transdifferentiation of HAoSMCs, next experiments explored the possible involvement of SGK1. As shown by Western blotting, treatment with exogenous bacterial sphingomyelinase significantly up-regulated SGK1 protein abundance in HAoSMCs at 30 min following treatment, levels remaining significantly increased up to 24 h following treatment (Figure 4A). Furthermore, exogenous ceramide supplementation significantly up-regulated SGK1 protein abundance in HAoSMCs (Figure 4B). To further determine whether SGK1 plays a role in osteo-/chondrogenic signaling promoted by bacterial sphingomyelinase and ceramide, the endogenous expression of SGK1 in HAoSMCs was suppressed by using small interfering RNA (siRNA) (Supplementary Figure S3). As shown in Figure 5A–C, the bacterial sphingomyelinase-induced *MSX2*, *CBFA1* and *ALPL* mRNA expression was significantly inhibited in SGK1-silenced HAoSMCs as compared with negative control siRNA-transfected HAoSMCs. Similarly, knockdown of SGK1 significantly blunted C2-ceramide-induced *MSX2*, *CBFA1* and *ALPL* mRNA expression in HAoSMCs (Figure 5D–F).

In addition, inhibition of Phosphoinositide 3-kinase (PI3K), a critical upstream kinase involved in SGK1 regulation, significantly suppressed bacterial sphingomyelinase- (Supplementary Figure S4) as well as C2-ceramide-induced (Supplementary Figure S5) osteogenic markers mRNA expression in HAoSMCs.

Taken together, SGK1-dependent osteoinductive signaling mediated, at least in part, osteo-/chondrogenic transdifferentiation of HAoSMCs triggered by ASM/ceramide *in vitro*.

Effects of ASM inhibition on phosphate-induced osteo-/chondrogenic transdifferentiation and calcification of HAoSMCs

Further experiments explored the role of ASM/ceramide in phosphate-induced vascular calcification *in vitro*. To this end, HAoSMCs were treated with high phosphate concentrations without and with additional treatment with the functional ASM inhibitors amitriptyline or fendiline. As illustrated in Figure 6, ASM inhibition with either amitriptyline or fendiline significantly suppressed phosphate-induced *SGK1* mRNA expression (Figure 6A) as well as osteogenic markers *MSX2*, *CBFA1* and *ALPL* mRNA expression (Figure 6B–D) in HAoSMCs. Moreover, the ASM inhibitors significantly reduced calcification of HAoSMCs promoted by calcification medium (Figure 6E). Treatment with ASM inhibitors alone did not significantly modify osteoinductive signaling or mineralization of HAoSMCs. Thus, ASM inhibition interfered with phosphate-induced *SGK1* expression, osteo-/chondrogenic transdifferentiation and calcification of VSMCs. In addition, treatment with ASM inhibitors failed to suppress the increase in *ALPL* mRNA expression triggered by overexpression of a constitutively active SGK1 (Supplementary Figure S6), further suggesting that SGK1 is a downstream mediator of ASM in the osteoinductive signaling in HAoSMCs.

Effects of ASM deficiency on phosphate-induced osteo-/chondrogenic transdifferentiation and calcification of MAoSMCs

To confirm the role of ASM/ceramide in phosphate-induced vascular calcification, additional *in vitro* experiments were performed in MAoSMCs isolated from $Asm^{+/+}$ and $Asm^{-/-}$ mice. Phosphate treatment significantly up-regulated *Sgk1* and osteogenic markers mRNA expression in $Asm^{+/+}$ MAoSMCs, effects significantly blunted in $Asm^{-/-}$ MAoSMCs (Figure 7A–D). Addition of exogenous bacterial sphingomyelinase to the cell culture medium restored the increased *Sgk1* and *Cbfa1* mRNA expression in phosphate-treated $Asm^{-/-}$ MAoSMCs as compared with $Asm^{-/-}$ MAoSMCs treated with phosphate alone. However, the effects of bacterial sphingomyelinase on *Msx2* and *Alpl* mRNA expression in phosphate-treated $Asm^{-/-}$ MAoSMCs did not reach statistical significance (P=0.18 and P=0.11, respectively).

Furthermore, treatment with calcification medium induced calcification of $Asm^{+/+}$ MAoSMCs, effects blunted in the $Asm^{-/-}$ MAoSMCs (Figure 7E,F). Additional treatment with bacterial sphingomyelinase restored the calcification response as determined by the calcium content in $Asm^{-/-}$ MAoSMCs treated with calcification medium (Figure 7F). Thus, ASM deficiency protected against phosphate-induced vascular calcification *in vitro*, while exogenous bacterial sphingomyelinase supplementation restored osteoinductive signaling and calcification of VSMCs during hyperphosphatemic conditions.

Clinical Science (2021) **135** 515–534
https://doi.org/10.1042/CS20201122

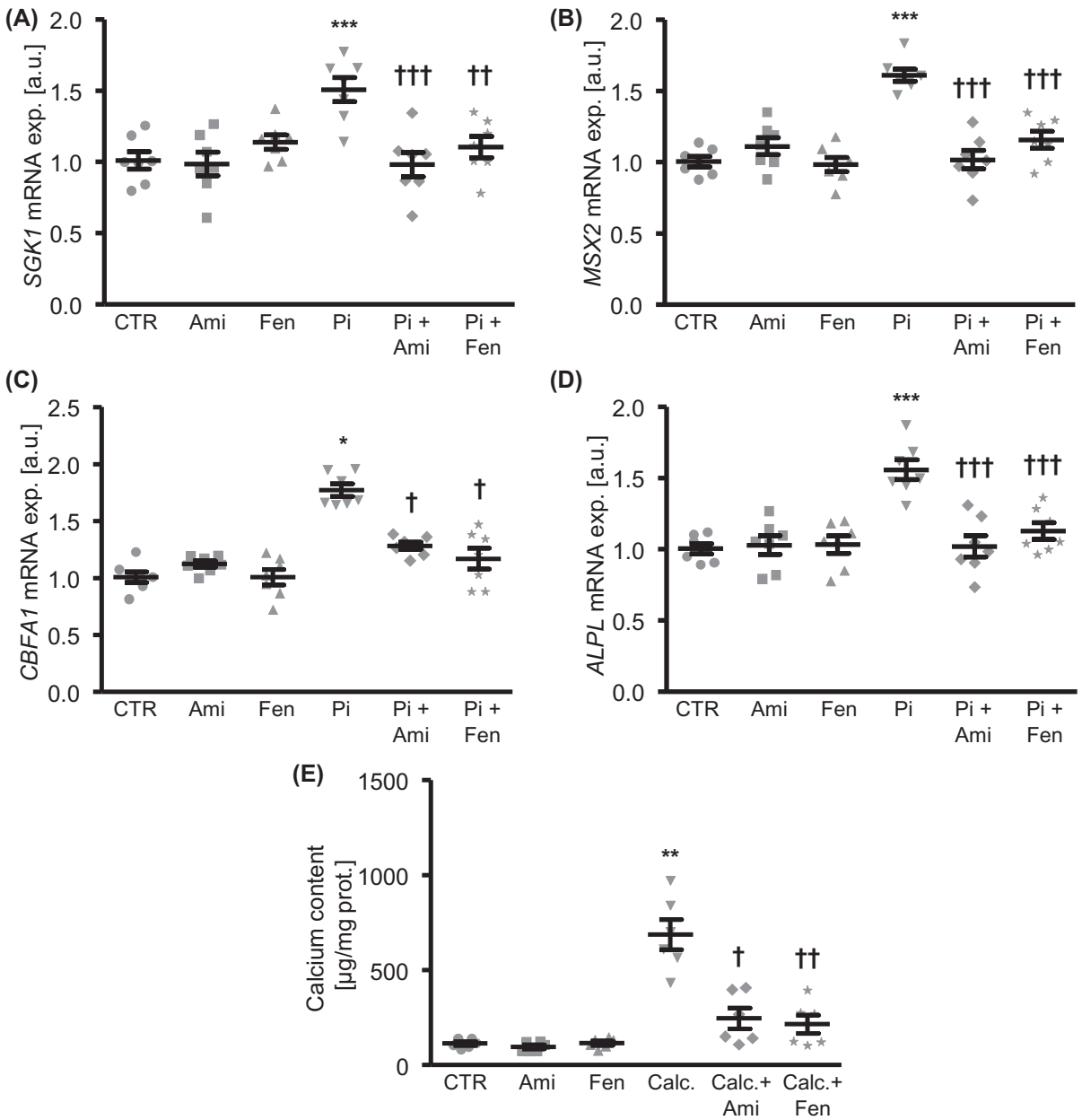

Figure 6. ASM inhibition suppresses phosphate-induced *SGK1* expression, osteo-/chondrogenic transdifferentiation and calcification of HAoSMCs

(**A–D**) Scatter dot plots and arithmetic means ± SEM (n=7; arbitrary units, a.u.) of *SGK1* (A), *MSX2* (B), *CBFA1* (C) and *ALPL* (D) relative mRNA expression in HAoSMCs following treatment for 24 h with control (CTR) or β-glycerophosphate (Pi) without or with additional treatment with amitriptyline (Ami) or fendiline (Fen). (**E**) Scatter dot plots and arithmetic means ± SEM (n=6; µg/mg protein) of calcium content in HAoSMCs following treatment for 11 days with control (CTR) or calcification medium (Calc.) without or with additional treatment with amitriptyline (Ami) or fendiline (Fen). *(P<0.05), **(P<0.01), ***(P<0.001) significant compared with control HAoSMCs; †(P<0.05), ††(P<0.01), †††(P<0.001) significant compared with Pi/Calc.-treated HAoSMCs.

Effects of Asm deficiency during cholecalciferol overload-induced vascular calcification in mice

To investigate the role of Asm in the regulation of vascular calcification *in vivo*, further experiments were performed in $Asm^{+/+}$ and $Asm^{-/-}$ mice following high-dosed cholecalciferol treatment. As a result, high-dosed cholecalciferol

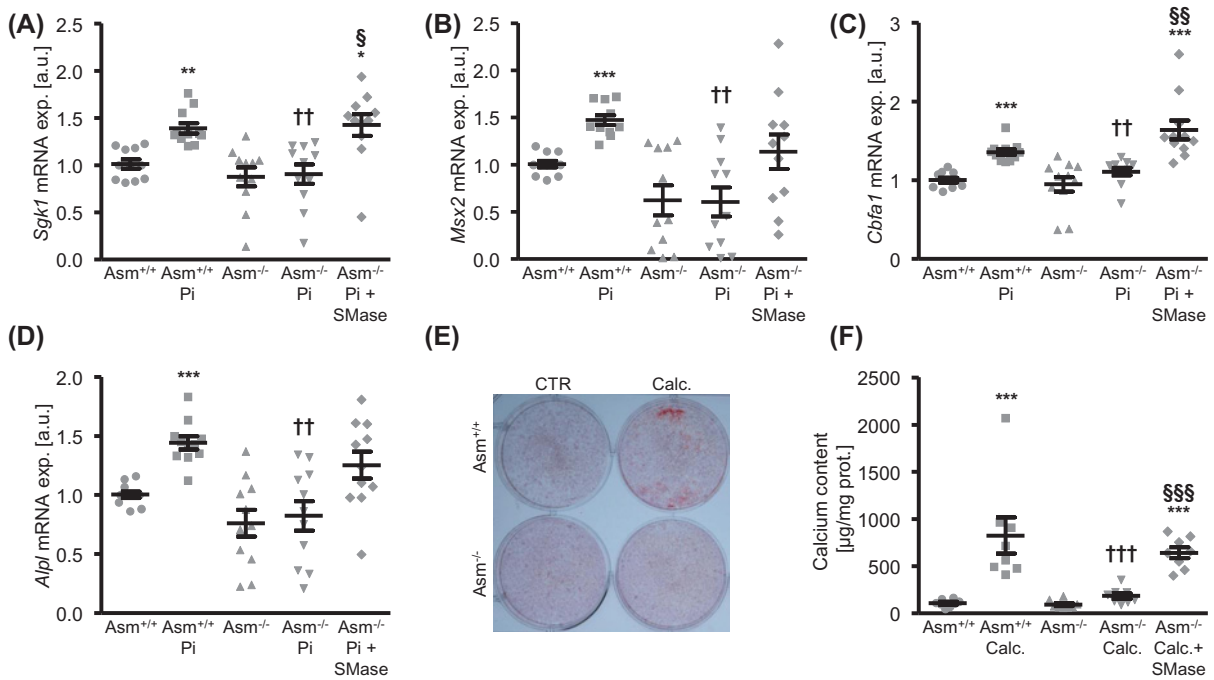

Figure 7. Asm deficiency reduces phosphate-induced *Sgk1* expression, osteo-/chondrogenic transdifferentiation and calcification of MAoSMCs

(**A–D**) Scatter dot plots and arithmetic means ± SEM (n=11; arbitrary units, a.u.) of *Sgk1* (A), *Msx2* (B), *Cbfa1* (C) and *Alpl* (D) relative mRNA expression in MAoSMCs isolated from $Asm^{+/+}$ and $Asm^{-/-}$ mice and following treatment for 24 h with control (CTR) or β-glycerophosphate (Pi) without or with bacterial sphingomyelinase (SMase). (**E**) Representative images showing Alizarin Red staining in MAoSMCs isolated from $Asm^{+/+}$ and $Asm^{-/-}$ mice and following treatment for 11 days with control (CTR) or calcification medium (Calc.). The calcified areas are shown as red. (**F**) Scatter dot plots and arithmetic means ± SEM (n=8; µg/mg protein) of calcium content in MAoSMCs isolated from $Asm^{+/+}$ and $Asm^{-/-}$ mice and following treatment for 11 days with control (CTR) or calcification medium (Calc.) without or with bacterial sphingomyelinase (SMase). *(P<0.05), **(P<0.01), ***(P<0.001) significant compared with control $Asm^{+/+}$ MAoSMCs; ††(P<0.01), †††(P<0.001) significant between Pi/Calc.-treated $Asm^{+/+}$ and $Asm^{-/-}$ MAoSMCs; §(P<0.05), §§(P<0.01), §§§(P<0.001) significant between Pi/Calc.- and Pi/Calc.+SMase-treated $Asm^{-/-}$ MAoSMCs.

significantly increased serum calcium concentrations in $Asm^{+/+}$ and $Asm^{-/-}$ mice as compared with control-treated mice, and did not significantly modify serum phosphate concentrations (Supplementary Table S1). Serum calcium (P=0.058) and phosphate (P=0.073) levels were not significantly different, but showed tendencies of altered levels between cholecalciferol-treated $Asm^{+/+}$ and $Asm^{-/-}$ mice (Supplementary Table S1). As shown by aortic Alizarin Red staining and quantification of calcium content in the aortic arch, high-dosed cholecalciferol induced vascular calcification in $Asm^{+/+}$ mice, effects suppressed in the $Asm^{-/-}$ mice (Figure 8A,B). These effects were paralleled by similar regulation of the osteoinductive signaling in aortic tissue. High-dosed cholecalciferol up-regulated aortic osteogenic markers *Msx2*, *Cbfa1* and *Alpl* mRNA expression in $Asm^{+/+}$ mice, but not in $Asm^{-/-}$ mice (Figure 8C–E). Moreover, the up-regulation of *Sgk1* mRNA expression after cholecalciferol treatment was significantly lower in aortic tissue of $Asm^{-/-}$ mice than of $Asm^{+/+}$ mice (Figure 8F). Thus, Asm deficiency reduced aortic *Sgk1* expression, osteo-/chondrogenic signaling and vascular calcification *in vivo* in the cholecalciferol-overload mouse model.

Effects of Asm deficiency on vascular calcification induced *ex vivo* in isolated-perfused mouse aortic tissue

To confirm the relevance of vascular Asm during vascular calcification, additional experiments were performed *ex vivo* in aortic tissue isolated from $Asm^{+/+}$ and $Asm^{-/-}$ mice and perfused with calcification medium. As illustrated in Figure 9A,B, calcium content after perfusion with calcification medium was significantly lower in aortic tissue isolated from $Asm^{-/-}$ mice than from $Asm^{+/+}$ mice. Similarly, the mRNA expression of *Msx2, Alpl* and *Sgk1* was significantly suppressed in isolated-perfused $Asm^{-/-}$ aortic tissue as compared with $Asm^{+/+}$ aortic tissue. However,

Clinical Science (2021) **135** 515–534
https://doi.org/10.1042/CS20201122

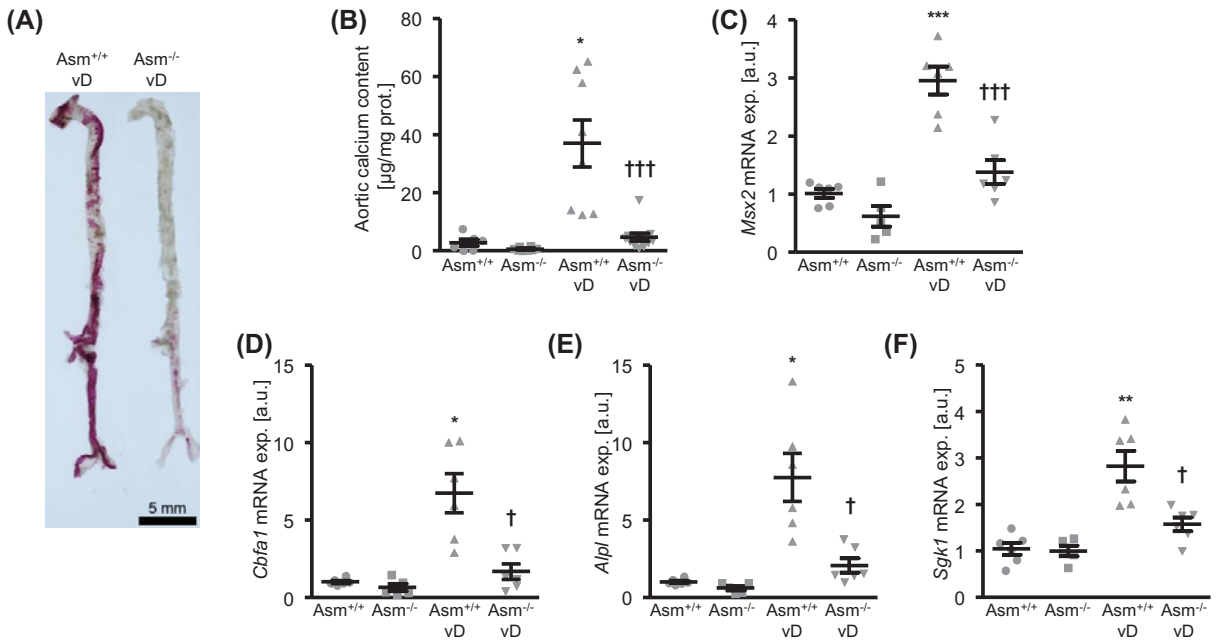

Figure 8. Asm deficiency ameliorates vascular calcification during cholecalciferol overload in mice

(**A**) Representative images showing aortic Alizarin Red staining in $Asm^{+/+}$ and $Asm^{-/-}$ mice receiving high-dosed cholecalciferol (vD). Scale bar: 5 mm. The calcified areas are shown as red. (**B**) Scatter dot plots and arithmetic means ± SEM (n=6–11; µg/mg protein) of calcium content in the aortic arch of $Asm^{+/+}$ and $Asm^{-/-}$ mice receiving vehicle or high-dosed cholecalciferol (vD). (**C–F**) Scatter dot plots and arithmetic means ± SEM (n=5-6; arbitrary units, a.u.) of *Msx2* (C), *Cbfa1* (D), *Alpl* (E) and *Sgk1* (F) relative mRNA expression in aortic tissue of $Asm^{+/+}$ and $Asm^{-/-}$ mice receiving vehicle or high-dosed cholecalciferol (vD). *(P<0.05), **(P<0.01), ***(P<0.001) significant compared with control $Asm^{+/+}$ mice; †(P<0.05), †††(P<0.001) significant compared with vD-treated $Asm^{+/+}$ mice.

the effects of Asm deficiency on *Cbfa1* mRNA expression in calcification medium-perfused arteries did not reach statistical significance (P=0.073, Figure 9C–F).

Effects of Asm inhibition during cholecalciferol overload-induced vascular calcification in mice

To confirm the pro-calcific role of Asm in development of vascular calcification *in vivo*, mice were treated with high-dosed cholecalciferol without or with the Asm inhibitors amitriptyline or fendiline. In mice, high-dosed cholecalciferol treatment significantly increased serum calcium concentrations and reduced serum phosphate levels, effects not significantly modified by treatment with Asm inhibitors (Supplementary Table S2). High-dosed cholecalciferol induced aortic calcification (Figure 10A) and up-regulated mRNA expression of aortic osteogenic markers *Msx2*, *Cbfa1* and *Alpl* (Figure 10B–D) as well as *Sgk1* (Figure 10E). All these effects were significantly reduced by additional treatment with amitriptyline or fendiline. Thus, Asm inhibition ameliorated vascular calcification in the cholecalciferol-overload mouse model.

Effects of ASM inhibition on uremic serum-induced osteo-/chondrogenic transdifferentiation of HAoSMCs

Next experiments analyzed the effects of ASM inhibition on osteo-/chondrogenic transdifferentiation of HAoSMCs during uremic conditions. HAoSMCs were exposed to uremic serum collected from hemodialysis patients and control serum from healthy volunteers [8] in the absence and presence of the ASM inhibitors amitriptyline or fendiline. Exposure to uremic serum significantly up-regulated *SGK1* and osteogenic markers mRNA expression in HAoSMCs as compared with control serum exposed HAoSMCs (Figure 11). All these effects were significantly reduced in the presence of ASM inhibitors. Thus, ASM inhibition interfered with osteoinductive signaling in HAoSMCs during exposure to uremic serum.

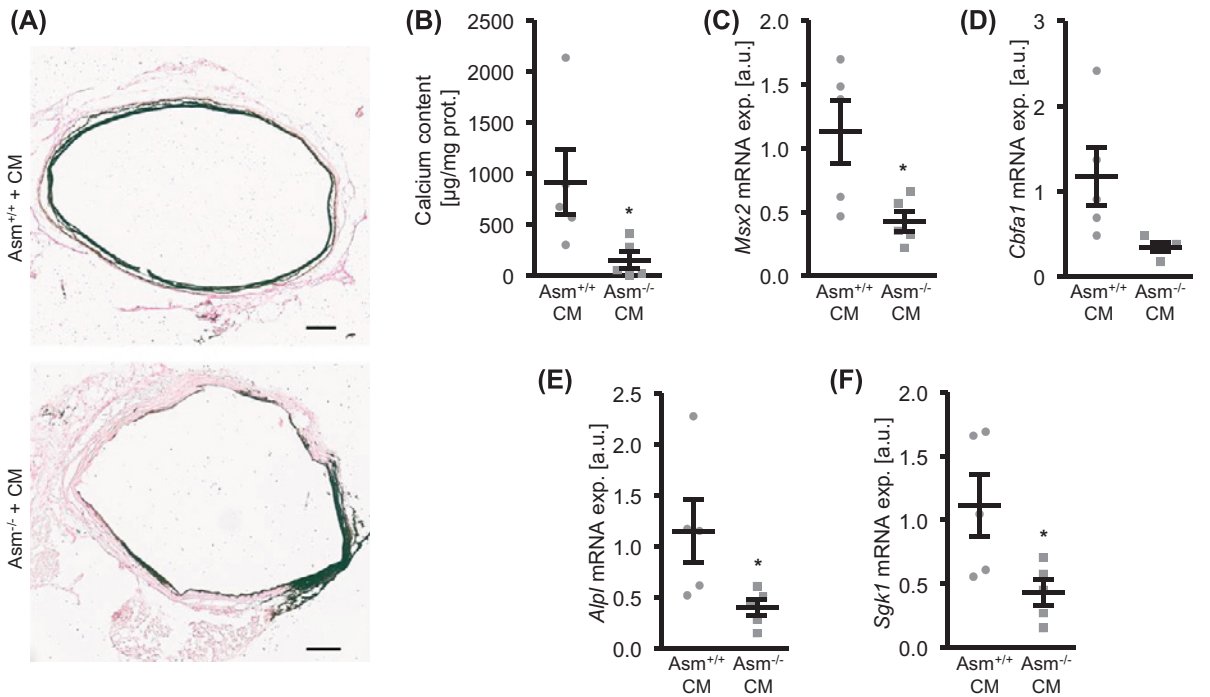

Figure 9. Asm deficiency suppresses osteo-/chondrogenic transdifferentiation and calcification of isolated-perfused mouse aortic tissue during exposure to calcification medium

(**A**) Representative images of Von Kossa staining in aortic tissue isolated from $Asm^{+/+}$ and $Asm^{-/-}$ mice and perfused *ex vivo* for 7 days with calcification medium (CM). Scale bar 100 μm. The calcified areas are shown as gray/black. (**B**) Scatter dot plots and arithmetic means ± SEM (n=5; μg/mg protein) of calcium content in aortic tissue isolated from $Asm^{+/+}$ and $Asm^{-/-}$ mice and perfused *ex vivo* with calcification medium (CM). (**C–F**) Scatter dot plots and arithmetic means ± SEM (n=5; arbitrary units, a.u.) of *Msx2* (C), *Cbfa1* (D), *Alpl* (E) and *Sgk1* (F) relative mRNA expression in aortic tissue isolated from $Asm^{+/+}$ and $Asm^{-/-}$ mice and perfused *ex vivo* for 7 days with calcification medium (CM). *(P<0.05) significant compared with CM-treated $Asm^{+/+}$ aortic tissue.

Discussion

The present study describes a key role of ASM/ceramide in the signaling events controlling vascular calcification. ASM and ceramide promote osteo-/chondrogenic transdifferentiation of VSMCs through an SGK1-dependent pathway and contribute to the progression of vascular calcification during elevated phosphate conditions. Furthermore, ASM deficiency or inhibition is able to interfere with phosphate-induced vascular calcification.

Supplementation of sphingomyelinase or ceramide is sufficient to induce osteo-/chondrogenic transdifferentiation of VSMCs *in vitro*. Accordingly, prolonged exposure to sphingomyelinase or ceramide augments VSMC calcification during pro-calcific conditions. Interestingly, deficiency of the calcification inhibitor magnesium was shown as sufficient to increase ceramide production in VSMCs [55]. Smooth muscle cell-specific overexpression of ASM augments vascular calcification *in vivo* [32]. Furthermore, ceramide treatment augments the effects of oxidized-LDL on vascular calcification [33,34]. On the other hand, in bovine VSMCs, ceramide treatment ameliorated calcification, but these diverging effects may be due to differing model systems [56]. Nonetheless, ASM-deficient VSMCs display a markedly blunted calcification response, which could be, at least partly, rescued by sphingomyelinase supplementation. Thus, the current observations indicate a critical role of ASM-derived ceramide signaling in the orchestration of VSMC osteo-/chondrogenic transdifferentiation.

Mechanistically, the present observations identify SGK1 as a downstream mediator of the pro-calcific effects of ASM and ceramide. SGK1 is a highly dynamically regulated kinase, and regulation of SGK1 activity involves transcriptional up-regulation, activation by PI3K and rapid proteasomal degradation [57]. SGK1 is typically expressed at low levels, but up-regulated during various pathological conditions [58]. Accordingly, SGK1 is up-regulated in VSMCs during pro-calcifying conditions [8] and SGK1 is required for triggering pro-calcific signaling during high phosphate, high glucose or interleukin-18 exposure [8,43,59]. SGK1 activates the transcription factor NF-κB to mediate at least

Clinical Science (2021) **135** 515–534
https://doi.org/10.1042/CS20201122

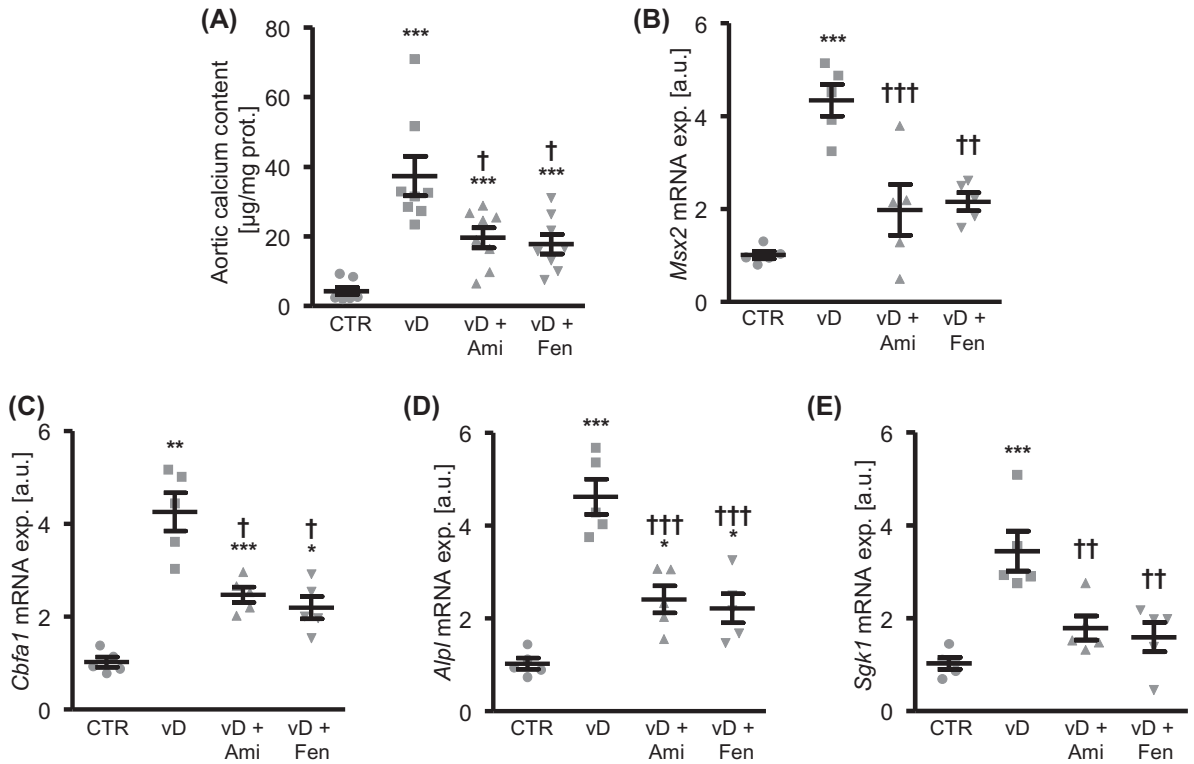

Figure 10. Asm inhibition reduces vascular calcification during cholecalciferol overload in mice

(**A**) Scatter dot plots and arithmetic means ± SEM (n=8; µg/mg protein) of calcium content in the aortic arch of mice receiving vehicle (CTR) or high-dosed cholecalciferol (vD) without or with additional treatment with amitriptyline (Ami) or fendiline (Fen). (**B–E**) Scatter dot plots and arithmetic means ± SEM (n=5; arbitrary units, a.u.) of *Msx2* (B), *Cbfa1* (C), *Alpl* (D) and *Sgk1* (E) relative mRNA expression in aortic tissue of mice receiving vehicle (CTR) or high-dosed cholecalciferol (vD) without or with additional treatment with amitriptyline (Ami) or fendiline (Fen). *(P<0.05), **(P<0.01), ***(P<0.001) significant compared with CTR mice; †(P<0.05), ††(P<0.01), †††(P<0.001) significant compared with vD-treated mice.

some of its pro-calcific effects [8], but the signaling events upstream of SGK1 were ill-defined. The current observations indicate that SGK1 is a downstream mediator of phosphate-induced pro-calcific ceramide signaling, since SGK1 knockdown suppresses the pro-calcific effects of sphingomyelinase and ceramide treatment in VSMCs. The pro-calcific effects of sphingomyelinase and ceramide were also blunted by wortmannin or LY294002, supporting an involvement of the PI3K pathway. Ceramide is known to block PKB/AKT activation by dephosphorylation at Ser^{473}, without reducing PI3K activity [60]. Ceramide treatment increases SGK1 in HEK293 cells, but inhibits AKT [61]. AKT plays a complex role in vascular calcification, and apparently is involved in an anti-calcific pathway [62], but is also associated with pro-calcific effects [63]. It is tempting to speculate that ASM-derived ceramide might modulate kinetics and direct pathways downstream of PI3K towards a pro-calcific signaling cascade.

However, the exact mechanism how ceramide interacts with components of the PI3K signaling pathway is unknown, since only very few proteins are known to directly interact with ceramide [64]. Also, discriminating effects of various ceramides and between the contribution of the two lysosomal and secreted isoforms of ASM to the effects of phosphate and other potential activators of ASM in the vasculature require further research [13]. Furthermore, other signaling pathways [33,65] and cellular processes [31–33,66] contributing to the effects of ASM on vascular calcification cannot be ruled out. ASM is able to induce cell apoptosis in VSMCs [66]. Apoptosis may promote vascular calcification by release of apoptotic bodies, which may act as nidus sites for calcium-phosphate precipitation [3]. Moreover, ASM is involved in the regulation of extracellular vesicle release [32,67], which could be a downstream effect of VSMC osteo-/chondrogenic transdifferentiation, but the underlying mechanisms require further study.

ASM deficiency is associated with blunted vascular calcification and mRNA expression of *Sgk1*, *Msx2*, *Cbfa1* and *Alpl in vivo* after mineral stress due to cholecalciferol overload. A tendency for alterations of serum calcium and

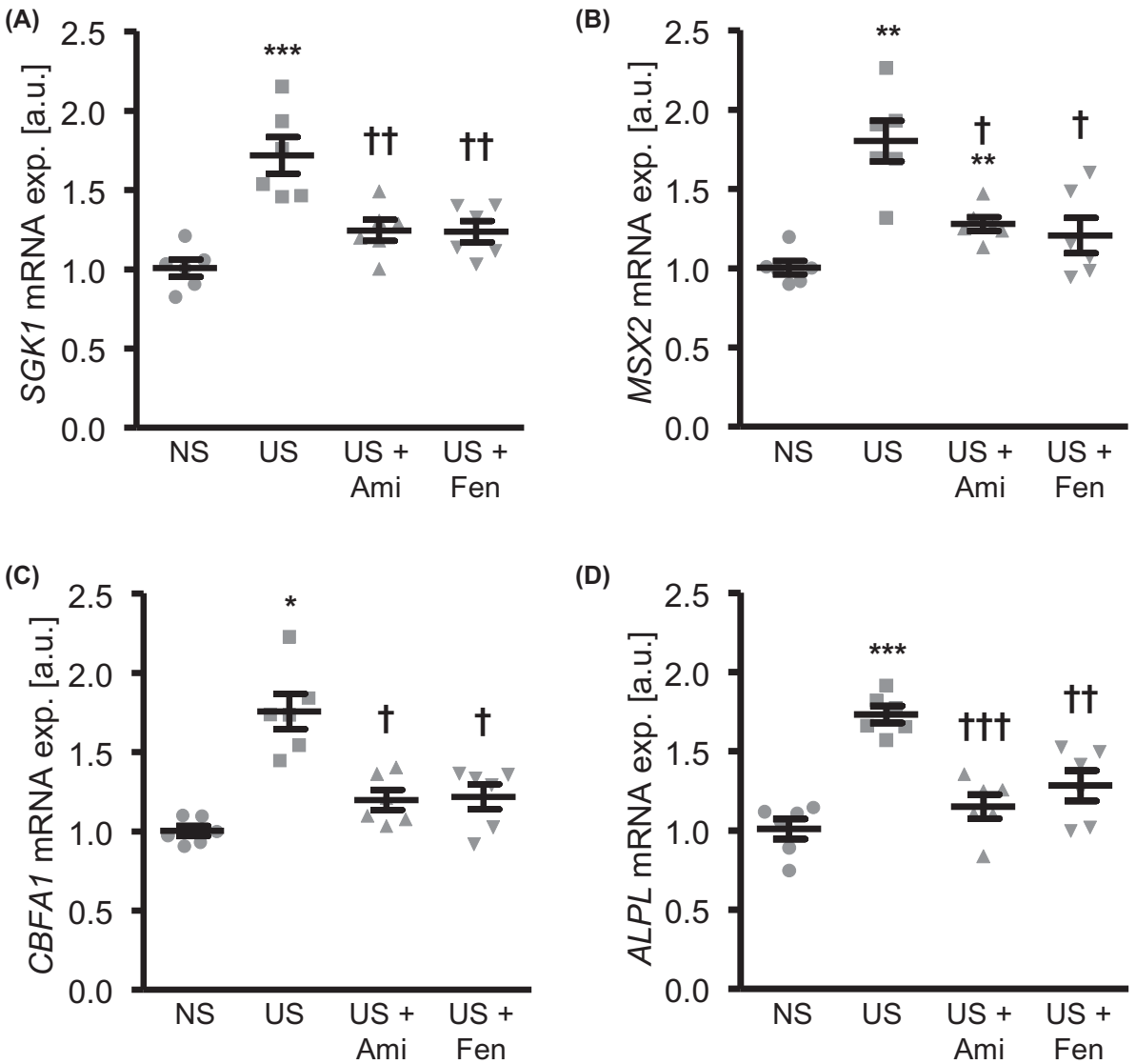

Figure 11. ASM inhibition blunts uremic serum-induced *SGK1* expression and osteo-/chondrogenic transdifferentiation of HAoSMCs

(**A–D**) Scatter dot plots and arithmetic means ± SEM (n=6; arbitrary units, a.u.) of *SGK1* (A), *MSX2* (B), *CBFA1* (C) and *ALPL* (D) relative mRNA expression in HAoSMCs following exposure for 24 h to 15% normal serum (NS) or uremic serum (US) without or with additional treatment with amitriptyline (Ami) or fendiline (Fen). *(P<0.05), **(P<0.01), ***(P<0.001) significant compared with NS-exposed HAoSMCs; †(P<0.05), ††(P<0.01), †††(P<0.001) significant compared with US-exposed HAoSMCs.

phosphate levels were noted between the genotypes during cholecalciferol overload and an effect of ASM on mineral homeostasis cannot be ruled out. However, the pro-calcific effects of ASM seem to be at least partly mediated in vascular tissue, since ASM deficiency also ameliorates calcification in an isolated-perfused artery model. Furthermore, treatment with either, the tricyclic antidepressant amitriptyline or the calcium channel blocker fendiline is able to blunt aortic calcification and expression of the osteogenic markers in the cholecalciferol-overload model without modifying serum calcium and phosphate levels. These distinct substances were both described as powerful functional inhibitors of ASM (FIASMA) [49]. Amitriptyline and fendiline are also effective in reducing osteo-/chondrogenic transdifferentiation of VSMCs during uremic conditions induced by treatment with serum from dialysis patients. These observations indicate ASM activity as a critical upstream activator inducing the pro-calcific pathways during CKD.

Clinical Science (2021) **135** 515–534
https://doi.org/10.1042/CS20201122

ASM deficiency or blockade has also been associated with beneficial vascular or renal effects in other models. ASM and ceramide are implicated in the development of endothelial dysfunction and atherosclerosis [65], as well as cardiac dysfunction [68]. ASM deficiency reduces the glomerular injury following hyperhomocysteinemia [69]. In a high-fat diet mouse model, amitriptyline treatment is able to reduce plasma ceramides and ameliorate renal injury [70]. Furthermore, anti-inflammatory properties described for amitriptyline treatment include blunted renal fibrosis and muscular inflammation in mice [71,72].

Clinical observations indicate a putative cardiovascular relevance of dysregulated ceramide. Ceramide levels are increased in children with CKD [73], and are associated with CKD in patients with ischemic heart disease [27]. In a hemodialysis cohort, higher plasma glucosylceramide (C16GC) is associated with increased mortality [74]. Moreover, associations of increased ceramide levels with cardiovascular events are observed in non-CKD populations [75–77].

The current observations suggest that pharmacological ASM blockade may provide beneficial effects on vascular calcification during CKD. A large group of clinically used pharmacological agents act as FIASMAs, including psychoanaleptics and antihistamines [78]. However, FIASMAs may require high lysosomal concentrations to inhibit ASM, questioning the relevant dosages of these agents in the human patients [78]. Also, the repurposing of FIASMAs may be limited by other effects of these drugs and should be carefully considered, as tricyclic antidepressants were shown to actually increase the risk for cardiovascular events in adults without known CKD [79]. The current observations, therefore, advocate a critical evaluation of putative benefits versus risks of FIASMA treatment in patients with CKD.

In conclusion, ASM/ceramide contributes to the development of vascular calcification during hyperphosphatemia by promoting SGK1-dependent osteo-/chondrogenic transdifferentiation of VSMCs. Thus, ASM may represent a therapeutic target to interfere with the progression of vascular calcification and to reduce the development of cardiovascular disease during hyperphosphatemic conditions such as CKD.

Clinical perspectives

- Phosphate-induced medial vascular calcification in CKD is associated with cardiovascular mortality, but no feasible treatment option exists. Vascular calcification is augmented by osteo-/chondrogenic transdifferentiation of VSMCs, but the mechanisms initiating a pro-calcific signaling cascade are still incompletely understood.
- This work describes the ASM as critical regulator of SGK1-dependent vascular osteo-/chondrogenic transdifferentiation during calcifying conditions. Most importantly, the FIASMAs, amitriptyline or fendiline are able to blunt vascular calcification in pre-clinical models.
- Therefore, repurposing routinely used medications with ASM-inhibiting properties for use in conditions of vascular calcification warrant further study.

Competing Interests

The authors declare that there are no competing interests associated with the manuscript.

Funding

This work was supported by the Deutsche Forschungsgemeinschaft [grant numbers AL2054/1-1, VO2259/2-1]; the Else Kröner-Fresenius-Stiftung [grant number 2017_A32]; the Berlin Institute of Health (BIH); the DZHK (German Centre for Cardiovascular Research); the Bundesministerium für Bildung und Forschung (BMBF) [grant number FKZ031L0231]; and the Charité 3R.

CRediT Author Contribution

Trang Thi Doan Luong: Conceptualization, Investigation, Writing — review and editing. **Rashad Tuffaha:** Investigation, Writing — review and editing. **Mirjam Schuchardt:** Funding acquisition, Investigation, Writing — review and editing. **Barbara Moser:** Investigation, Writing — review and editing. **Nadeshda Schelski:** Investigation, Writing — review and editing. **Beate Boehme:** Investigation, Writing — review and editing. **Can Gollmann-Tepeköylü:** Conceptualization, Writing — review and editing. **Clara Schramm:** Investigation, Writing — review and editing. **Johannes Holfeld:** Conceptualization, Writing — review and editing.

Burkert Pieske: Conceptualization, Writing — review and editing. **Erich Gulbins:** Conceptualization, Writing — review and editing. **Markus Tölle:** Funding acquisition, Conceptualization, Writing — review and editing. **Markus van der Giet:** Conceptualization, Writing — review and editing. **Florian Lang:** Conceptualization, Writing — review and editing. **Kai-Uwe Eckardt:** Conceptualization, Writing — review and editing. **Jakob Voelkl:** Conceptualization, Funding acquisition, Writing — original draft, Writing — review and editing. **Ioana Alesutan:** Conceptualization, Funding acquisition, Investigation, Writing — original draft, Writing — review and editing.

Acknowledgements

The authors gratefully acknowledge the technical assistance of M. Kiminezhadmalaie and the Advanced Medical Bioimaging Core Facility (AMBIO) of the Charité for support in acquisition of the imaging data.

Abbreviations

ALP, alkaline phosphatase; ASM, acid sphingomyelinase; BSA, bovine serum albumin; CBFA1, core-binding factor α1; FIASMA, functional inhibitors of ASM; GAPDH, glyceraldehyde-3-phosphate dehydrogenase; HAoSMC, human aortic smooth muscle cell; MAoSMC, mouse aortic smooth muscle cell; MSX2, msh homeobox 2; NF-κB, nuclear factor κ-light-chain-enhancer of activated B cell; NS, normal serum; PI3K, Phosphoinositide 3-kinase; siRNA, small interfering RNA; SGK1, serum- and glucocorticoid-inducible kinase 1; US, uremic serum; VSMC, vascular smooth muscle cell.

References

1 Ebert, T., Pawelzik, S.C., Witasp, A., Arefin, S., Hobson, S., Kublickiene, K. et al. (2020) Inflammation and premature ageing in chronic kidney disease. *Toxins (Basel)* **12** (4), 227, https://doi.org/10.3390/toxins12040227
2 Voelkl, J., Cejka, D. and Alesutan, I. (2019) An overview of the mechanisms in vascular calcification during chronic kidney disease. *Curr. Opin. Nephrol. Hypertens.* **28**, 289–296, https://doi.org/10.1097/MNH.0000000000000507
3 Voelkl, J., Lang, F., Eckardt, K.U., Amann, K., Kuro, O.M., Pasch, A. et al. (2019) Signaling pathways involved in vascular smooth muscle cell calcification during hyperphosphatemia. *Cell. Mol. Life Sci.* **76**, 2077–2091
4 Lang, F., Ritz, E., Voelkl, J. and Alesutan, I. (2013) Vascular calcification–is aldosterone a culprit? *Nephrol. Dial. Transplant.* **28**, 1080–1084, https://doi.org/10.1093/ndt/gft041
5 Alves, R.D., Eijken, M., van de Peppel, J. and van Leeuwen, J.P. (2014) Calcifying vascular smooth muscle cells and osteoblasts: independent cell types exhibiting extracellular matrix and biomineralization-related mimicries. *BMC Genomics* **15**, 965, https://doi.org/10.1186/1471-2164-15-965
6 Lang, F., Leibrock, C., Pelzl, L., Gawaz, M., Pieske, B., Alesutan, I. et al. (2018) Therapeutic interference with vascular calcification-lessons from klotho-hypomorphic mice and beyond. *Front. Endocrinol. (Lausanne)* **9**, 207, https://doi.org/10.3389/fendo.2018.00207
7 Dai, L., Schurgers, L.J., Shiels, P.G. and Stenvinkel, P. (2020) Early vascular ageing in chronic kidney disease: impact of inflammation, vitamin K, senescence and genomic damage. *Nephrol. Dial. Transplant.* **35**, ii31–ii37, https://doi.org/10.1093/ndt/gfaa006
8 Voelkl, J., Luong, T.T., Tuffaha, R., Musculus, K., Auer, T., Lian, X. et al. (2018) SGK1 induces vascular smooth muscle cell calcification through NF-kappaB signaling. *J. Clin. Invest.* **128**, 3024–3040, https://doi.org/10.1172/JCI96477
9 Ewence, A.E., Bootman, M., Roderick, H.L., Skepper, J.N., McCarthy, G., Epple, M. et al. (2008) Calcium phosphate crystals induce cell death in human vascular smooth muscle cells: a potential mechanism in atherosclerotic plaque destabilization. *Circ. Res.* **103**, e28–e34, https://doi.org/10.1161/CIRCRESAHA.108.181305
10 Alesutan, I., Musculus, K., Castor, T., Alzoubi, K., Voelkl, J. and Lang, F. (2015) Inhibition of phosphate-induced vascular smooth muscle cell osteo-/chondrogenic signaling and calcification by bafilomycin A1 and methylamine. *Kidney Blood Press. Res.* **40**, 490–499, https://doi.org/10.1159/000368524
11 Gatt, S. (1963) Enzymic hydrolysis and synthesis of ceramides. *J. Biol. Chem.* **238**, 3131–3133, https://doi.org/10.1016/S0021-9258(18)51879-2
12 Marchesini, N. and Hannun, Y.A. (2004) Acid and neutral sphingomyelinases: roles and mechanisms of regulation. *Biochem. Cell. Biol.* **82**, 27–44, https://doi.org/10.1139/o03-091
13 Pavoine, C. and Pecker, F. (2009) Sphingomyelinases: their regulation and roles in cardiovascular pathophysiology. *Cardiovasc. Res.* **82**, 175–183, https://doi.org/10.1093/cvr/cvp030
14 Andrews, N.W. (2019) Solving the secretory acid sphingomyelinase puzzle: Insights from lysosome-mediated parasite invasion and plasma membrane repair. *Cell. Microbiol.* **21**, e13065, https://doi.org/10.1111/cmi.13065
15 Maceyka, M. and Spiegel, S. (2014) Sphingolipid metabolites in inflammatory disease. *Nature* **510**, 58–67, https://doi.org/10.1038/nature13475
16 Grassme, H., Riethmuller, J. and Gulbins, E. (2007) Biological aspects of ceramide-enriched membrane domains. *Prog. Lipid Res.* **46**, 161–170, https://doi.org/10.1016/j.plipres.2007.03.002
17 Hannun, Y.A. and Obeid, L.M. (2018) Sphingolipids and their metabolism in physiology and disease. *Nat. Rev. Mol. Cell Biol.* **19**, 175–191, https://doi.org/10.1038/nrm.2017.107
18 Cogolludo, A., Villamor, E., Perez-Vizcaino, F. and Moreno, L. (2019) Ceramide and regulation of vascular tone. *Int. J. Mol. Sci.* **20** (2), 411, https://doi.org/10.3390/ijms20020411
19 Del Gaudio, I., Sasset, L., Lorenzo, A.D. and Wadsack, C. (2020) Sphingolipid signature of human feto-placental vasculature in preeclampsia. *Int. J. Mol. Sci.* **21**, https://doi.org/10.3390/ijms21031019

20 Yu, Z., Peng, Q. and Huang, Y. (2019) Potential therapeutic targets for atherosclerosis in sphingolipid metabolism. *Clin. Sci. (Lond.)* **133**, 763–776, https://doi.org/10.1042/CS20180911
21 Su, Y.T., Cheng, Y.P., Zhang, X., Xie, X.P., Chang, Y.M. and Bao, J.X. (2020) Acid sphingomyelinase/ceramide mediates structural remodeling of cerebral artery and small mesenteric artery in simulated weightless rats. *Life Sci.* **243**, 117253, https://doi.org/10.1016/j.lfs.2019.117253
22 Bao, J.X., Chang, H., Lv, Y.G., Yu, J.W., Bai, Y.G., Liu, H. et al. (2012) Lysosome-membrane fusion mediated superoxide production in hyperglycaemia-induced endothelial dysfunction. *PLoS ONE* **7**, e30387, https://doi.org/10.1371/journal.pone.0030387
23 Lankinen, M., Schwab, U., Kolehmainen, M., Paananen, J., Nygren, H., Seppanen-Laakso, T. et al. (2015) A healthy nordic diet alters the plasma lipidomic profile in adults with features of metabolic syndrome in a multicenter randomized dietary intervention. *J. Nutr.* **146**, 662–672, https://doi.org/10.3945/jn.115.220459
24 Laaksonen, R., Ekroos, K., Sysi-Aho, M., Hilvo, M., Vihervaara, T., Kauhanen, D. et al. (2016) Plasma ceramides predict cardiovascular death in patients with stable coronary artery disease and acute coronary syndromes beyond LDL-cholesterol. *Eur. Heart J.* **37**, 1967–1976, https://doi.org/10.1093/eurheartj/ehw148
25 Mantovani, A. and Dugo, C. (2020) Ceramides and risk of major adverse cardiovascular events: A meta-analysis of longitudinal studies. *J. Clin. Lipidol.* **14**, 176–185, https://doi.org/10.1016/j.jacl.2020.01.005
26 Tarasov, K., Ekroos, K., Suoniemi, M., Kauhanen, D., Sylvanne, T., Hurme, R. et al. (2014) Molecular lipids identify cardiovascular risk and are efficiently lowered by simvastatin and PCSK9 deficiency. *J. Clin. Endocrinol. Metab.* **99**, E45–E52, https://doi.org/10.1210/jc.2013-2559
27 Mantovani, A., Lunardi, G., Bonapace, S., Dugo, C., Altomari, A., Molon, G. et al. (2020) Association between increased plasma ceramides and chronic kidney disease in patients with and without ischemic heart disease. *Diabetes Metab.*, https://doi.org/10.1016/j.diabet.2020.03.003
28 Devlin, C.M., Leventhal, A.R., Kuriakose, G., Schuchman, E.H., Williams, K.J. and Tabas, I. (2008) Acid sphingomyelinase promotes lipoprotein retention within early atheromata and accelerates lesion progression. *Arterioscler. Thromb. Vasc. Biol.* **28**, 1723–1730, https://doi.org/10.1161/ATVBAHA.108.173344
29 Jiang, M., Huang, S., Duan, W., Liu, Q. and Lei, M. (2019) Inhibition of acid sphingomyelinase activity ameliorates endothelial dysfunction in db/db mice. *Biosci. Rep.* **39** (4), https://doi.org/10.1042/BSR20182144
30 Leger, A.J., Mosquea, L.M., Li, L., Chuang, W., Pacheco, J., Taylor, K. et al. (2011) Adeno-associated virus-mediated expression of acid sphingomyelinase decreases atherosclerotic lesion formation in apolipoprotein E(-/-) mice. *J. Gene Med.* **13**, 324–332, https://doi.org/10.1002/jgm.1575
31 Li, X., Xu, M., Pitzer, A.L., Xia, M., Boini, K.M., Li, P.L. et al. (2014) Control of autophagy maturation by acid sphingomyelinase in mouse coronary arterial smooth muscle cells: protective role in atherosclerosis. *J. Mol. Med. (Berl.)* **92**, 473–485, https://doi.org/10.1007/s00109-014-1120-y
32 Bhat, O.M., Yuan, X., Cain, C., Salloum, F.N. and Li, P.L. (2020) Medial calcification in the arterial wall of smooth muscle cell-specific Smpd1 transgenic mice: a ceramide-mediated vasculopathy. *J. Cell. Mol. Med.* **24**, 539–553, https://doi.org/10.1111/jcmm.14761
33 Liao, L., Zhou, Q., Song, Y., Wu, W., Yu, H., Wang, S. et al. (2013) Ceramide mediates Ox-LDL-induced human vascular smooth muscle cell calcification via p38 mitogen-activated protein kinase signaling. *PLoS ONE* **8**, e82379, https://doi.org/10.1371/journal.pone.0082379
34 Song, Y., Hou, M., Li, Z., Luo, C., Ou, J.S., Yu, H. et al. (2017) TLR4/NF-kappaB/Ceramide signaling contributes to Ox-LDL-induced calcification of human vascular smooth muscle cells. *Eur. J. Pharmacol.* **794**, 45–51, https://doi.org/10.1016/j.ejphar.2016.11.029
35 Henze, L.A., Luong, T.T.D., Boehme, B., Masyout, J., Schneider, M.P., Brachs, S. et al. (2019) Impact of C-reactive protein on osteo-/chondrogenic transdifferentiation and calcification of vascular smooth muscle cells. *Aging (Albany N.Y.)* **11**, 5445–5462, https://doi.org/10.18632/aging.102130
36 Luong, T.T.D., Estepa, M., Boehme, B., Pieske, B., Lang, F., Eckardt, K.U. et al. (2019) Inhibition of vascular smooth muscle cell calcification by vasorin through interference with TGFbeta1 signaling. *Cell. Signal.* **64**, 109414, https://doi.org/10.1016/j.cellsig.2019.109414
37 Alesutan, I., Luong, T.T.D., Schelski, N., Masyout, J., Hille, S., Schneider, M.P. et al. (2020) Circulating uromodulin inhibits vascular calcification by interfering with pro-inflammatory cytokine signaling. *Cardiovasc. Res.* cvaa081, https://doi.org/10.1093/cvr/cvaa081
38 Voelkl, J., Castor, T., Musculus, K., Viereck, R., Mia, S., Feger, M. et al. (2015) SGK1-sensitive regulation of cyclin-dependent kinase inhibitor 1B (p27) in cardiomyocyte hypertrophy. *Cell. Physiol. Biochem.* **37**, 603–614, https://doi.org/10.1159/000430380
39 Munzer, P., Borst, O., Walker, B., Schmid, E., Feijge, M.A., Cosemans, J.M. et al. (2014) Acid sphingomyelinase regulates platelet cell membrane scrambling, secretion, and thrombus formation. *Arterioscler. Thromb. Vasc. Biol.* **34**, 61–71, https://doi.org/10.1161/ATVBAHA.112.300210
40 Voelkl, J., Alesutan, I., Leibrock, C.B., Quintanilla-Martinez, L., Kuhn, V., Feger, M. et al. (2013) Spironolactone ameliorates PIT1-dependent vascular osteoinduction in klotho-hypomorphic mice. *J. Clin. Invest.* **123**, 812–822
41 Voelkl, J., Tuffaha, R., Luong, T.T.D., Zickler, D., Masyout, J., Feger, M. et al. (2018) Zinc inhibits phosphate-induced vascular calcification through TNFAIP3-mediated suppression of NF-kappaB. *J. Am. Soc. Nephrol.* **29**, 1636–1648, https://doi.org/10.1681/ASN.2017050492
42 Alesutan, I., Feger, M., Tuffaha, R., Castor, T., Musculus, K., Buehling, S.S. et al. (2016) Augmentation of phosphate-induced osteo-/chondrogenic transformation of vascular smooth muscle cells by homoarginine. *Cardiovasc. Res.* **110**, 408–418, https://doi.org/10.1093/cvr/cvw062
43 Schelski, N., Luong, T.T.D., Lang, F., Pieske, B., Voelkl, J. and Alesutan, I. (2019) SGK1-dependent stimulation of vascular smooth muscle cell osteo-/chondrogenic transdifferentiation by interleukin-18. *Pflugers Arch.* **471**, 889–899, https://doi.org/10.1007/s00424-019-02256-5
44 Horinouchi, K., Erlich, S., Perl, D.P., Ferlinz, K., Bisgaier, C.L., Sandhoff, K. et al. (1995) Acid sphingomyelinase deficient mice: a model of types A and B Niemann-Pick disease. *Nat. Genet.* **10**, 288–293, https://doi.org/10.1038/ng0795-288
45 Santana, P., Pena, L.A., Haimovitz-Friedman, A., Martin, S., Green, D., McLoughlin, M. et al. (1996) Acid sphingomyelinase-deficient human lymphoblasts and mice are defective in radiation-induced apoptosis. *Cell* **86**, 189–199, https://doi.org/10.1016/S0092-8674(00)80091-4
46 Alesutan, I., Tuffaha, R., Auer, T., Feger, M., Pieske, B., Lang, F. et al. (2017) Inhibition of osteo/chondrogenic transformation of vascular smooth muscle cells by MgCl2 via calcium-sensing receptor. *J. Hypertens.* **35**, 523–532, https://doi.org/10.1097/HJH.0000000000001202
47 Price, P.A., Buckley, J.R. and Williamson, M.K. (2001) The amino bisphosphonate ibandronate prevents vitamin D toxicity and inhibits vitamin D-induced calcification of arteries, cartilage, lungs and kidneys in rats. *J. Nutr.* **131**, 2910–2915, https://doi.org/10.1093/jn/131.11.2910

48 Price, P.A., Faus, S.A. and Williamson, M.K. (2000) Warfarin-induced artery calcification is accelerated by growth and vitamin D. *Arterioscler. Thromb. Vasc. Biol.* **20**, 317–327, https://doi.org/10.1161/01.ATV.20.2.317
49 Gulbins, E., Palmada, M., Reichel, M., Luth, A., Bohmer, C., Amato, D. et al. (2013) Acid sphingomyelinase-ceramide system mediates effects of antidepressant drugs. *Nat. Med.* **19**, 934–938, https://doi.org/10.1038/nm.3214
50 Alesutan, I., Voelkl, J., Feger, M., Kratschmar, D.V., Castor, T., Mia, S. et al. (2017) Involvement of vascular aldosterone synthase in phosphate-induced osteogenic transformation of vascular smooth muscle cells. *Sci. Rep.* **7**, 2059, https://doi.org/10.1038/s41598-017-01882-2
51 Schuchardt, M., Siegel, N.V., Babic, M., Reshetnik, A., Lutzenberg, R., Zidek, W. et al. (2020) A novel long-term ex vivo model for studying vascular calcification pathogenesis: the rat isolated-perfused aorta. *J. Vasc. Res.* **57**, 46–52, https://doi.org/10.1159/000503785
52 Wang, X. and Seed, B. (2003) A PCR primer bank for quantitative gene expression analysis. *Nucleic Acids Res.* **31**, e154, https://doi.org/10.1093/nar/gng154
53 Krishnamurthy, K., Dasgupta, S. and Bieberich, E. (2007) Development and characterization of a novel anti-ceramide antibody. *J. Lipid Res.* **48**, 968–975, https://doi.org/10.1194/jlr.D600043-JLR200
54 Tuffaha, R., Voelkl, J., Pieske, B., Lang, F. and Alesutan, I. (2018) Role of PKB/SGK-dependent phosphorylation of GSK-3alpha/beta in vascular calcification during cholecalciferol overload in mice. *Biochem. Biophys. Res. Commun.* **503**, 2068–2074, https://doi.org/10.1016/j.bbrc.2018.07.161
55 Altura, B.M., Shah, N.C., Shah, G.J., Li, W., Zhang, A., Zheng, T. et al. (2013) Magnesium deficiency upregulates sphingomyelinases in cardiovascular tissues and cells: cross-talk among proto-oncogenes, Mg(2+), NF-kappaB and ceramide and their potential relationships to resistant hypertension, atherogenesis and cardiac failure. *Int. J. Clin. Exp. Med.* **6**, 861–879
56 Morris, T.G., Borland, S.J., Clarke, C.J., Wilson, C., Hannun, Y.A., Ohanian, V. et al. (2018) Sphingosine 1-phosphate activation of ERM contributes to vascular calcification. *J. Lipid Res.* **59**, 69–78, https://doi.org/10.1194/jlr.M079731
57 Lang, F., Stournaras, C., Zacharopoulou, N., Voelkl, J. and Alesutan, I. (2018) Serum- and glucocorticoid-inducible kinase 1 and the response to cell stress. *Cell Stress* **3**, 1–8, https://doi.org/10.15698/cst2019.01.170
58 Lang, F. and Voelkl, J. (2013) Therapeutic potential of serum and glucocorticoid inducible kinase inhibition. *Expert Opin. Investig. Drugs* **22**, 701–714, https://doi.org/10.1517/13543784.2013.778971
59 Poetsch, F., Henze, L.A., Estepa, M., Moser, B., Pieske, B., Lang, F. et al. (2020) Role of SGK1 in the osteogenic transdifferentiation and calcification of vascular smooth muscle cells promoted by hyperglycemic conditions. *Int. J. Mol. Sci.* **21** (19), 7207, https://doi.org/10.3390/ijms21197207
60 Schubert, K.M., Scheid, M.P. and Duronio, V. (2000) Ceramide inhibits protein kinase B/Akt by promoting dephosphorylation of serine 473. *J. Biol. Chem.* **275**, 13330–13335, https://doi.org/10.1074/jbc.275.18.13330
61 Pastore, D., Della-Morte, D., Coppola, A., Capuani, B., Lombardo, M.F., Pacifici, F. et al. (2015) SGK-1 protects kidney cells against apoptosis induced by ceramide and TNF-alpha. *Cell Death Dis.* **6**, e1890, https://doi.org/10.1038/cddis.2015.232
62 Ponnusamy, A., Sinha, S., Hyde, G.D., Borland, S.J., Taylor, R.F., Pond, E. et al. (2018) FTI-277 inhibits smooth muscle cell calcification by up-regulating PI3K/Akt signaling and inhibiting apoptosis. *PLoS ONE* **13**, e0196232, https://doi.org/10.1371/journal.pone.0196232
63 Byon, C.H., Javed, A., Dai, Q., Kappes, J.C., Clemens, T.L., Darley-Usmar, V.M. et al. (2008) Oxidative stress induces vascular calcification through modulation of the osteogenic transcription factor Runx2 by AKT signaling. *J. Biol. Chem.* **283**, 15319–15327, https://doi.org/10.1074/jbc.M800021200
64 Zeidan, Y.H. and Hannun, Y.A. (2010) The acid sphingomyelinase/ceramide pathway: biomedical significance and mechanisms of regulation. *Curr. Mol. Med.* **10**, 454–466, https://doi.org/10.2174/156652410791608225
65 Bismuth, J., Lin, P., Yao, Q. and Chen, C. (2008) Ceramide: a common pathway for atherosclerosis? *Atherosclerosis* **196**, 497–504, https://doi.org/10.1016/j.atherosclerosis.2007.09.018
66 Loidl, A., Sevcsik, E., Riesenhuber, G., Deigner, H.P. and Hermetter, A. (2003) Oxidized phospholipids in minimally modified low density lipoprotein induce apoptotic signaling via activation of acid sphingomyelinase in arterial smooth muscle cells. *J. Biol. Chem.* **278**, 32921–32928
67 Bhat, O.M., Li, G., Yuan, X., Huang, D., Gulbins, E., Kukreja, R.C. et al. (2020) Arterial medial calcification through enhanced small extracellular vesicle release in smooth muscle-specific Asah1. *Gene Knockout Mice. Sci. Rep.* **10**, 1645
68 Park, M.H., Jin, H.K. and Bae, J.S. (2020) Potential therapeutic target for aging and age-related neurodegenerative diseases: the role of acid sphingomyelinase. *Exp. Mol. Med.* **52**, 380–389, https://doi.org/10.1038/s12276-020-0399-8
69 Boini, K.M., Xia, M., Li, C., Zhang, C., Payne, L.P., Abais, J.M. et al. (2011) Acid sphingomyelinase gene deficiency ameliorates the hyperhomocysteinemia-induced glomerular injury in mice. *Am. J. Pathol.* **179**, 2210–2219, https://doi.org/10.1016/j.ajpath.2011.07.019
70 Boini, K.M., Zhang, C., Xia, M., Poklis, J.L. and Li, P.L. (2010) Role of sphingolipid mediator ceramide in obesity and renal injury in mice fed a high-fat diet. *J. Pharmacol. Exp. Ther.* **334**, 839–846, https://doi.org/10.1124/jpet.110.168815
71 Achar, E., Maciel, T.T., Collares, C.F., Teixeira, V.P. and Schor, N. (2009) Amitriptyline attenuates interstitial inflammation and ameliorates the progression of renal fibrosis. *Kidney Int.* **75**, 596–604, https://doi.org/10.1038/ki.2008.578
72 Manning, J., Kulbida, R., Rai, P., Jensen, L., Bouma, J., Singh, S.P. et al. (2014) Amitriptyline is efficacious in ameliorating muscle inflammation and depressive symptoms in the mdx mouse model of Duchenne muscular dystrophy. *Exp. Physiol.* **99**, 1370–1386, https://doi.org/10.1113/expphysiol.2014.079475
73 Mitsnefes, M., Scherer, P.E., Friedman, L.A., Gordillo, R., Furth, S., Warady, B.A. et al. (2014) Ceramides and cardiac function in children with chronic kidney disease. *Pediatr. Nephrol.* **29**, 415–422, https://doi.org/10.1007/s00467-013-2642-1
74 Mitsnefes, M.M., Fitzpatrick, J., Sozio, S.M., Jaar, B.G., Estrella, M.M., Monroy-Trujillo, J.M. et al. (2018) Plasma glucosylceramides and cardiovascular risk in incident hemodialysis patients. *J. Clin. Lipidol.* **12**, 1513.e4–1522.e4, https://doi.org/10.1016/j.jacl.2018.07.011
75 Meeusen, J.W., Donato, L.J., Bryant, S.C., Baudhuin, L.M., Berger, P.B. and Jaffe, A.S. (2018) Plasma ceramides. *Arterioscler. Thromb. Vasc. Biol.* **38**, 1933–1939, https://doi.org/10.1161/ATVBAHA.118.311199

Clinical Science (2021) **135** 515–534
https://doi.org/10.1042/CS20201122

76 Mundra, P.A., Barlow, C.K., Nestel, P.J., Barnes, E.H., Kirby, A., Thompson, P. et al. (2018) Large-scale plasma lipidomic profiling identifies lipids that predict cardiovascular events in secondary prevention. *JCI Insight* **3**, https://doi.org/10.1172/jci.insight.121326

77 Wang, D.D., Toledo, E., Hruby, A., Rosner, B.A., Willett, W.C., Sun, Q. et al. (2017) Plasma Ceramides, mediterranean diet, and incident cardiovascular disease in the PREDIMED Trial (Prevencion con Dieta Mediterranea). *Circulation* **135**, 2028–2040, https://doi.org/10.1161/CIRCULATIONAHA.116.024261

78 Kornhuber, J., Tripal, P., Reichel, M., Muhle, C., Rhein, C., Muehlbacher, M. et al. (2010) Functional Inhibitors of Acid Sphingomyelinase (FIASMAs): a novel pharmacological group of drugs with broad clinical applications. *Cell. Physiol. Biochem.* **26**, 9–20, https://doi.org/10.1159/000315101

79 Hamer, M., Batty, G.D., Seldenrijk, A. and Kivimaki, M. (2011) Antidepressant medication use and future risk of cardiovascular disease: the Scottish Health Survey. *Eur. Heart J.* **32**, 437–442, https://doi.org/10.1093/eurheartj/ehq438

Acid sphingomyelinase promotes SGK1-dependent vascular calcification

Supplementary material

Supplementary Tables

Suppl. Table 1. Effect of Asm deficiency during cholecalciferol overload. Arithmetic means ± SEM of plasma calcium and phosphate concentrations in $Asm^{+/+}$ and $Asm^{-/-}$ mice receiving vehicle or high-dosed cholecalciferol (vD). ***(p<0.001) significant compared to control $Asm^{+/+}$ mice.

	$Asm^{+/+}$	**$Asm^{-/-}$**	**$Asm^{+/+}$ vD**	**$Asm^{-/-}$ vD**	
Calcium [mg/dl]	8.9 ± 0.4	9.1 ± 0.2	19.6 ± 1.0 ***	16.2 ± 0.5 ***	n=6-8
Phosphate [mg/dl]	8.5 ± 0.7	8.3 ± 0.7	7.5 ± 0.3	10.2 ± 1.1	n=6-8

Suppl. Table 2. Effect of Asm inhibition during cholecalciferol overload. Arithmetic means ± SEM of plasma calcium and phosphate concentrations in mice receiving vehicle (CTR) or high-dosed cholecalciferol (vD) without or with additional treatment with amitriptyline (Ami) or fendiline (Fen). *(p<0.05), **(p<0.01), ***(p<0.001) significant compared to CTR mice.

	CTR	**vD**	**vD + Ami**	**vD + Fen**	
Calcium [mg/dl]	8.1 ± 0.2	22.8 ± 1.0 ***	21.2 ± 0.7 ***	21.3 ± 1.4 ***	n=7
Phosphate [mg/dl]	7.8 ± 0.1	6.5 ± 0.4 *	6.4 ± 0.3 **	6.3 ± 0.2 **	n=7

Supplementary Figures

Suppl. Figure 1. Phosphate increases ceramide abundance in HAoSMCs. Representative histograms of flow cytometry analysis and scatter dot plots and arithmetic means ± SEM (n=6; arbitrary units, a.u.) of normalized ceramide-dependent fluorescence intensity in HAoSMCs following treatment for 24 hours with control (CTR), bacterial sphingomyelinase (SMase) or β-glycerophosphate (Pi). Negative controls are performed by omitting incubation with primary antibody and with primary and secondary antibodies, respectively. *($p<0.05$) significant compared to control HAoSMCs.

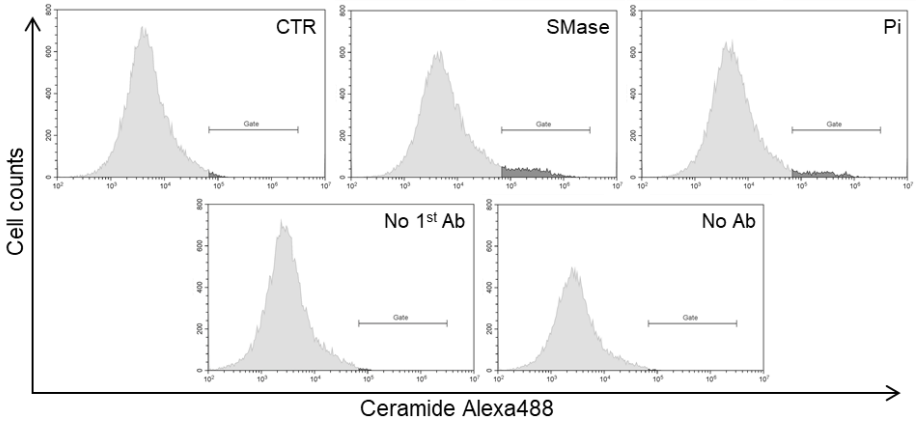

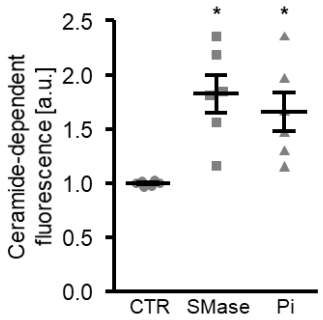

Suppl. Figure 2. ASM and ceramide increase apoptotic signalling in HAoSMCs. A. Scatter dot plots and arithmetic means ± SEM (n=8; arbitrary units, a.u.) of *BAX/BCL2* relative mRNA expression ratio in HAoSMCs following treatment for 24 hours with control (CTR) or bacterial sphingomyelinase (SMase). **B**. Scatter dot plots and arithmetic means ± SEM (n=6; a.u.) of *BAX/BCL2* relative mRNA expression ratio in HAoSMCs following treatment for 24 hours with control (CTR) or C2-ceramide (C2-cer). ***($p<0.001$) significant compared to control HAoSMCs.

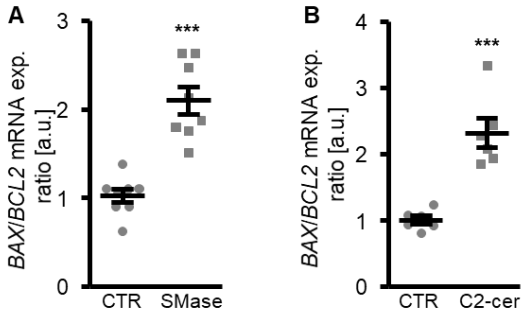

Suppl. Figure 3. *SGK1* gene silencing efficiency in HAoSMCs. A. Scatter dot plots and arithmetic means ± SEM (n=6; arbitrary units, a.u.) of *SGK1* relative mRNA expression in HAoSMCs following transfection with negative control siRNA (Neg.si) or SGK1 siRNA (SGK1si) and treatment for 24 hours with control or bacterial sphingomyelinase (SMase). **B**. Scatter dot plots and arithmetic means ± SEM (n=6; a.u.) of *SGK1* relative mRNA expression in HAoSMCs following transfection with negative control siRNA (Neg.si) or SGK1 siRNA (SGK1si) and treatment for 24 hours with control or C2-ceramide (C2-cer). ***(p<0.001) significant compared to Neg.si-transfected HAoSMCs.

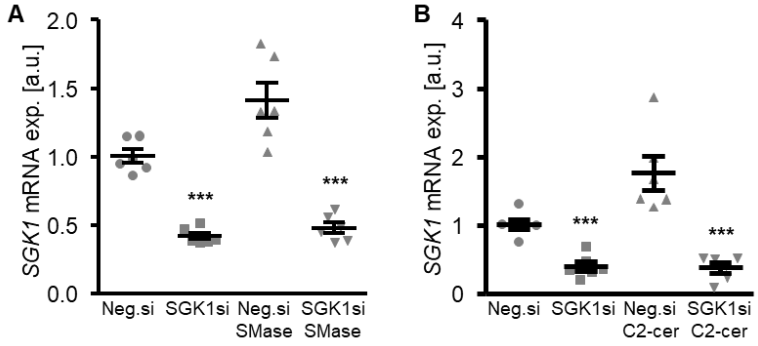

Suppl. Figure 4. PI3K inhibition suppresses ASM-induced osteo-/chondrogenic transdifferentiation of HAoSMCs. A-C. Scatter dot plots and arithmetic means ± SEM (n=6; arbitrary units, a.u.) of *MSX2* (**A**), *CBFA1* (**B**) and *ALPL* (**C**) relative mRNA expression in HAoSMCs following treatment for 24 hours with control (CTR) or bacterial sphingomyelinase (SMase) without or with additional treatment with PI3K inhibitors wortmannin (Wo) or LY294002 (LY). ***(p<0.001) significant compared to control HAoSMCs; †(p<0.05), ††(p<0.01), †††(p<0.001) significant compared to SMase-treated HAoSMCs.

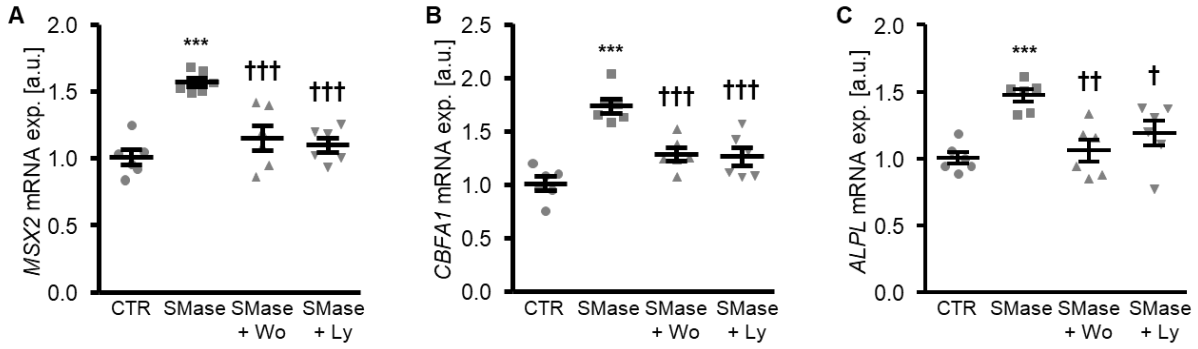

Suppl. Figure 5. PI3K inhibition suppresses ceramide-induced osteo-/chondrogenic transdifferentiation of HAoSMCs. A-C. Scatter dot plots and arithmetic means ± SEM (n=6; arbitrary units, a.u.) of *MSX2* (**A**), *CBFA1* (**B**) and *ALPL* (**C**) relative mRNA expression in HAoSMCs following treatment for 24 hours with control (CTR) or C2-ceramide (C2-cer) without or with additional treatment with PI3K inhibitors wortmannin (Wo) or LY294002 (LY). *(p<0.05), **(p<0.01), ***(p<0.001) significant compared to control HAoSMCs; ††(p<0.01), †††(p<0.001) significant compared to C2-cer-treated HAoSMCs.

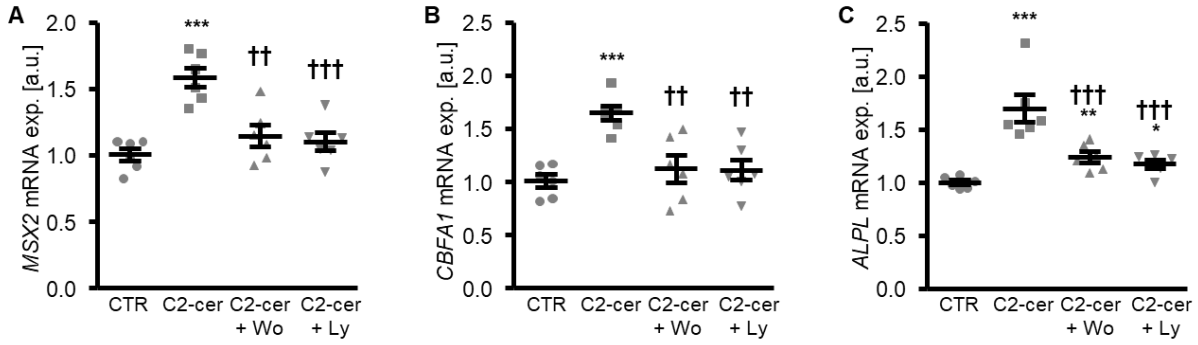

Suppl. Figure 6. ASM inhibition fails to reduce osteo-/chondrogenic transdifferentiation of HAoSMCs induced by overexpression of constitutively active SGK1. A,B. Scatter dot plots and arithmetic means ± SEM (n=7; arbitrary units, a.u.) of *SGK1* (**A**) and *ALPL* (**B**) relative mRNA expression in HAoSMCs following transfection with empty vector (V) or constitutively active SGK1^{S422D} (SGK1^{SD}) without or with additional treatment for 24 hours with amitriptyline (Ami) or fendiline (Fen). *($p<0.05$), **($p<0.01$) significant compared to V-transfected HAoSMCs.